Investigation of Narrow-Width Cuffs for Wearable Upper-Arm Oscillometric Monitoring of Blood Pressure

By

Asha Karmen-Chan

A Thesis

Submitted to the Faculty of

WORCESTER POLYTECHNIC INSTITUTE

In partial fulfillment of the requirements for the

Degree of Master of Science

in

Mechanical Engineering

August 16, 2023

APPROVED:

_____

Professor Yihao Zheng, Advisor
Mechanical and Materials Engineering Department, Worcester Polytechnic Institute

_____

Professor Quan Zhang, Co-Advisor
Department of Psychiatry, Massachusetts General Hospital/Harvard Medical School

_____

Professor Ahmet Can Sabuncu, Committee Member
Mechanical and Materials Engineering Department, Worcester Polytechnic Institute

_____

Professor Lin Cheng, Graduate Committee Representative
Mechanical and Materials Engineering Department, Worcester Polytechnic Institute

Acknowledgement

I would like to express my heartfelt gratitude to the following people for their support and direction as I completed my thesis:

At Massachusetts General Hospital: My advisor, Dr. Quan Zhang, for his instruction, suggestions, and abundant knowledge of electrical design–and for welcoming me to MGH as a part of the Neural Systems group in the Biomedical Engineering Lab; Dr. Mohamed Almadi for his perspective and patience as I learned my way around the lab; and Haoran Zhang, for providing valuable discussions and helping me realize my ideas in Matlab.

At Worcester Polytechnic Institute: My advisor, Dr. Yihao Zheng, introduced me to my colleagues at MGH and supported me as I conducted research in the WPI MedMain lab and completed my undergraduate Major Qualifying Project in a related blood pressure monitoring project. I am grateful for his invaluable feedback, attention to detail, and grasp of technical presentation. Thanks also to my committee members, Dr. Ahmet Sabuncu and Dr. Lin Cheng, for their knowledge, commentary, and approach to reviewing my work.

Lastly, I thank my family and friends for their unrelenting support and encouragement, and their generosity in assisting me as I navigated between Worcester and Boston.

This work was supported was supported by the National Institute of Biomedical Imaging and Bioengineering of the National Institutes of Health under award number R01EB027122. The content is solely the responsibility of the authors and does not necessarily represent the official views of the National Institutes of Health.

Abstract

Blood pressure (BP) is one of the four vital signs used to assess the clinical situation of a patient. Abnormalities in BP can be indicative of underlying conditions and serious illnesses. There are two standard ways of measuring BP in a clinical environment: arterial catheterization and oscillometry. Arterial catheterization is an invasive procedure that provides beat-to-beat BP readings. Oscillometric BP measurement is a non-invasive inflatable-cuff-based measurement that provides intermittent BP readings. Multiple shortcomings associated with current BP technology have prompted a new wave of research focused on wearable, non-invasive, continuous BP monitoring. Wearable, continuous BP monitoring has significant potential for both ambulatory and in-hospital care. It has the capacity to improve at-home monitoring and management of hypertension and to enable earlier detection and intervention during in-hospital clinical deterioration. In clinical settings wearable technology could also significantly reduce nursing workload and improve the frequency of intermittent BP measurement. Wearable BP systems are relatively simple, but estimation of BP is complicated by issues with sensor positioning and can be distorted by unpredictable interactions with the cardiovascular, respiratory, and autonomic nervous systems. Because of these complications, current wearable technologies are not standard for in-hospital use.

To improve wearable BP systems, this study proposes modifications to the oscillometric method for upper arm BP measurement; in the past, this avenue has been overlooked for creating wearable technology. The oscillometric cuff is a clinically-acceptable simple and standard method for measuring BP in both clinical and ambulatory settings. Modifications to the standard oscillometric cuff could allow for wearable, cuff-based BP monitoring. This study examines the feasibility of a narrow BP cuff for low-profile, wearable BP measurement. To assess feasibility,

three BP estimation algorithms were compared and corrected to justify the use of a narrow-width cuff for wearable devices. If a low-volume cuff could be fabricated it would permit a faster inflation and deflation period compared to the standard oscillometric cuff. This could minimize patient discomfort during BP measurement, increase response clinician response time to changes in BP, and reduce rest time between BP readings. With these capabilities, a wearable oscillometric cuff could provide a method for near-continuous, wearable BP measurement.

Table of Contents

Table of Figures

Table of Tables

1 Introduction

Blood pressure (BP) is one of the four vital signs used to assess the clinical situation of a patient. It is regularly monitored in in-hospital clinical environments and routine physical examinations, but the development of inexpensive monitoring devices also allows for BP to be measured in ambulatory settings (Johns Hopkins, 2017). Blood pressure is assessed as the pressure that circulating blood exerts on the walls of blood vessels during a cardiac cycle. The measurement is expressed in units of millimeters mercury (mmHg) as a ratio of systolic (SBP) to diastolic pressure (DBP). Systolic BP reflects the maximum pressure during one heartbeat and DBP reflects the minimum pressure between two heartbeats (Barral & Croibier, 2011).

Abnormalities in BP can be indicative of underlying conditions and serious illnesses. In routine physical examinations, BP is primarily measured to screen for hypertension, hypotension and response to antihypertensive medications (Muntner, Einhorn, et al., 2019). Hypertension (raised BP) affects nearly half of all adults in the U.S. and does not present with any obvious symptoms. Hypertension is the leading risk factor for cardiovascular disease (CVD), and CVD is the leading cause of death in the U.S. and worldwide (Fuchs & Whelton, 2020). In in-hospital clinical environments, such as perioperative care, change in BP is an indicator for clinical deterioration. Without intervention, clinical deterioration can progress to adverse consequences and/or death (Downey et al., 2018; Prgomet et al., 2016).

Routine BP measurement is the only way to detect hypertension and a critical way of detecting clinical deterioration. Intervention and management of these conditions is reliant on frequent BP monitoring due to the natural volatility of BP. For hypertensive patients, accurate diagnosis and management depends on daily at-home BP monitoring (Eguchi et al., 2009; Green

et al., 2022; Pickering et al., 2005). For in-hospital patients, early detection of clinical deterioration depends on near-continuous BP monitoring.

There are two standard ways of measuring BP in a clinical environment: arterial catheterization and oscillometry (Muntner, Shimbo, et al., 2019; Pickering et al., 2005; Roerecke et al., 2019). Arterial catheterization is an invasive procedure that provides beat-to-beat BP readings. Oscillometric BP measurement is a non-invasive inflatable-cuff-based measurement that provides intermittent BP readings. (Oscillometric BP is also the type of measurement used to assess ambulatory BP.) Multiple shortcomings with current BP technology have prompted a new wave of research focused on wearable, non-invasive, continuous BP monitoring (Chung et al., 2013; Fortin et al., 2021; Leenen et al., 2020).

Wearable, continuous BP monitoring has significant potential for both ambulatory and in-hospital care. Wearable technology has the potential to improve at-home monitoring and management of hypertension and enable earlier detection and intervention during in-hospital clinical deterioration. In clinical settings, wearable technology could also significantly reduce nursing workload and improve the frequency of intermittent BP measurement. Because vital sign measurement is a significant portion of nursing workload, vital measurements, like BP, are often measured below the frequency requested by the ordering provider (McDaniel & Ralston, 2022).

Studies on wearable BP systems have assessed a variety of methods for measuring BP. Most of these systems estimate BP using time (and occasionally amplitude) information gathered from photo-plethysmographic (PPG) and piezoelectric sensors (Chung et al., 2013; Fortin et al., 2021; Sharma et al., 2017; Yi et al., 2022). Wearable BP systems are relatively simple, but estimation of BP is complicated by issues with sensor positioning, and can be distorted by interactions with the cardiovascular, respiratory, and autonomic nervous systems (Mukkamala et

al., 2015; Rastegar et al., 2019). Overcoming these issues with BP measurement requires frequent calibration of wearable BP monitors with traditional oscillometric BP cuffs. This limits the usefulness of these monitors as wearable devices. Because of these complications, current wearable technologies are not standard for in-hospital use due to lack of clinical accuracy and excessive need for calibration.

To improve upon wearable BP systems, this study proposes that the oscillometric method for BP measurement is overlooked as a wearable technology. The oscillometric cuff is a simple and standard method for measuring BP in both clinical and ambulatory settings and is clinically accurate. Modification of the standard oscillometric cuff could allow for wearable, cuff-based BP monitoring. This study examines the feasibility of a narrow BP cuff for low-profile, wearable BP measurement. If a low-volume cuff could be fabricated it would permit a faster inflation and deflation period compared to the standard oscillometric cuff. This could minimize patient discomfort during BP measurement, increase response clinician response time to changes in BP, and reduce rest time between BP readings. With these capabilities, a wearable oscillometric cuff could provide a method for near-continuous, wearable BP measurement.

2 Background

Comprehension of the physiology of BP and the current methods for oscillometric measurement of BP are essential for development of wearable cuff-based technology. Adaptation of the traditional oscillometric cuff is dependent on the ability to address concerns with modification of cuff size, primarily via demonstration of accurate measurement algorithms.

2.1 Physiology of Blood Pressure

Blood pressure is the force that circulating blood exerts on the artery walls. The pressure is determined by the volume of circulating blood in the artery and compliance of the arterial walls. These variables are dependent on cardiac output and peripheral resistance which constantly fluctuate with each cardiac cycle. During the cardiac cycle, blood pressure increases as the heart empties (ventricular systole) and decreases as the heart fills (ventricular diastole). These two phases are assessed as SBP and DBP, respectively (Figure 2-1).

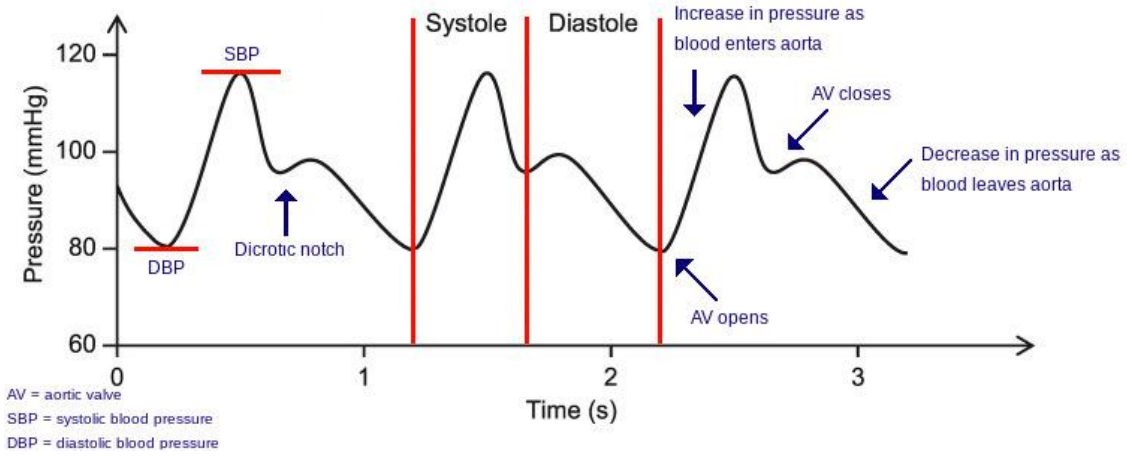

Figure 2-1. Blood pressure waveform. (Nguyen & Bora, 2023)

The SBP is dependent on cardiac output, elasticity of the large arteries, and the viscosity of the blood. The DBP is dependent on the speed of blood flow (which is controlled by peripheral resistance). The values of SBP and DBP fluctuate daily, but SBP is more prone to fluctuation than DBP because it is dependent on more variables (Barral & Croibier, 2011). Assessing BP through the components of SBP and DBP is important because they can be indicative of different conditions and they vary with age (Pickering et al., 2005; Strandberg & Pitkala, 2003). The SBP and DBP both increase with aging, but DBP plateaus around age 50 and

SBP continues to rise. This makes DBP a more potent cardiovascular risk factor than SBP for individuals under the age of 50 and SBP more important for individuals over the age of 50 (Chobanian et al., 2003). Pulse pressure (PP), calculated as $SBP - DBP$, is also a considerable risk factor for individuals over 60 years of age (Franklin et al., 2001). Both components of BP are primarily used to screen for hypertension, which is defined by the American Heart Association (AHA) in the table below:

Table 2-1. Table 1. Categories of BP in adults (Whelton et al., 2018)

BP Category	SBP	DBP
Normal	< 20 mmHg	< 80 mmHg
Elevated	120 – 129 mmHg	< 80 mmHg
Hypertension		
Stage 1	130 – 139 mmHg	80 – 90 mmHg
Stage 2	≥ 140 mmHg	≥ 90 mmHg

2.2 Oscillometry

Oscillometry is the most common method used for assessing BP (Sharman et al., 2023). In this method, a cuff is wrapped around a limb and inflated to occlude the artery. For most automated devices, occlusion is performed on the brachial artery, at the midpoint of the bicep. Blood pressure can be assessed during inflation or deflation of the cuff, but commercial devices customarily estimate BP during deflation. As the cuff is deflated, the pressure in the cuff is monitored for cardiac contractions (expressed as oscillations in cuff pressure) (Berger, 2001; Lewis et al., 2019). Oscillations appear when the cuff pressure drops below the SBP and blood resumes flowing through the artery. When the pressure drops below the DBP, oscillations in cuff pressure will cease as blood flow is uninterrupted. Blood pressure estimation is based on interpretation of the oscillations.

2.2.1 Manual Oscillometric Blood Pressure Estimation

Manual oscillometry is considered the gold standard for non-invasive BP measurement. Manual estimation is performed using a sphygmomanometer and requires auscultation. A sphygmomanometer has three components: a BP cuff, a pressure meter (mercury manometer or aneroid gauge), and a stethoscope. The technique for manual estimation was established in 1905 by Nikolai Korotkov, a Russian military surgeon who developed a five-phase auscultation-based procedure for determining BP (Shevchenko & Tsitlik, 1996). In this procedure, a trained operator manually inflates a BP cuff and listens for heartbeats during cuff deflation, known as Korotkoff sounds. There are five distinct Korotkoff sounds (heard sequentially during deflation) that are indicative of the type of flow in the artery (Ogedegbe & Pickering, 2010). Trained operators can listen to the Korotkoff sounds and distinguish SBP and DBP during deflation. Improper placement of cuff/stethoscope, noise distractions, and inattention, can alter manual estimation of BP. Manual estimation is considered the gold standard despite issues with human error because it more closely matches pressure measured invasively from an intra-arterial line (Babadag & Zaybak, 2021; Campbell & Pillarisetty, 2019).

2.2.2 Automatic Oscillometric Blood Pressure Estimation

Modern oscillometry employs the use of automated, electric systems to inflate and deflate a BP cuff and estimate BP. These devices can be operated by the patient and used in noisy environments. The exact method of BP estimation differs between automated oscillometric devices. Typically, automated cuffs will either inflate to approximately 20 mmHg over the SBP or inflate to a standard pressure and then begin deflation (Berger, 2001; Sharman et al., 2023). The pressure of the cuff is measured using a transducer that can detect small variations in pulse

pressure. Recorded oscillations in cuff pressure are analyzed using BP algorithms based on empirical data (Chandrasekhar et al., 2019; Drzewiecki et al., 1994). Because BP algorithms are empirical, there are many documented issues with improper calibration and misestimation of BP (Zheng et al., 2009). To address issues with clinical accuracy, the U.S. maintains a registry of validated oscillometric devices that meet specific American and European standards for BP measurement (Stergiou et al., 2019).

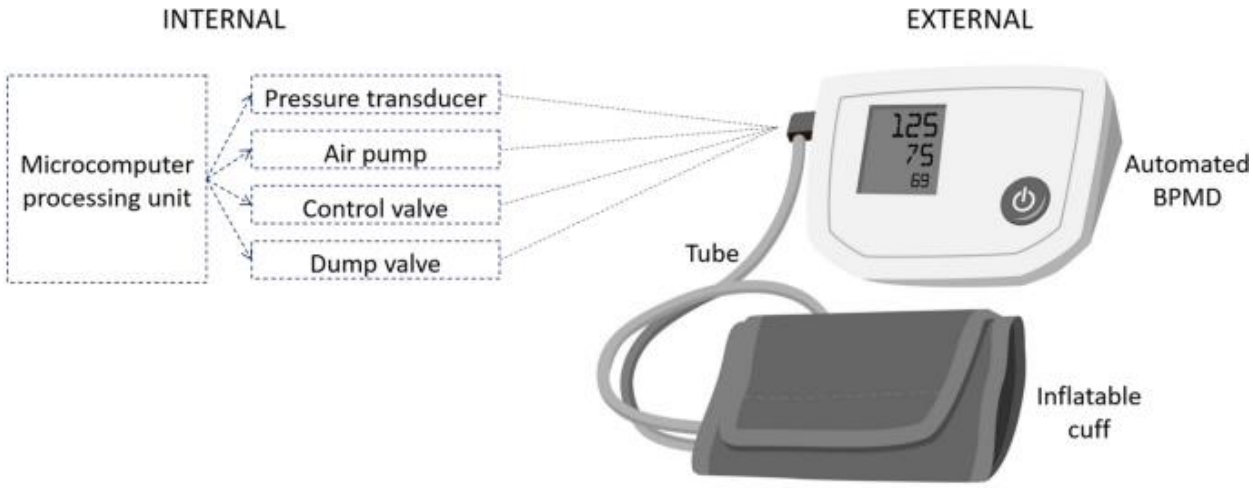

Figure 2-2. Summary of components for the operation of an automated blood pressure measurement device using the oscillometric method. (Sharman et al., 2023)

2.3 Standards for the Validation of Oscillometric Devices

Non-invasive blood pressure measurement is regulated by universal standards. These standards stipulate rules for clinical evaluation and validation of BP monitoring systems, but notably, not all BP systems are validated. Because of the low-risk classification of BP monitors, they can be distributed without validation. Multiple registries of validated BP systems exist (such as the international registries StrideBP and Medaval) to help address discrepancies between BP systems (Picone et al., 2020; Stergiou et al., 2019). For validated systems, the European Society of Hypertension (ESH), the American National Standards Institute (ANSI), Association for the

Advancement of Medical Instrumentation (AAMI), and the International Organization for Standardization (ISO) jointly publish requirements for non-invasive sphygmomanometers under the standard "ANSI/AAMI/ISO 81060". This standard applies to all human populations and all conditions of use (i.e., clinical, ambulatory, etc.) and specifies requirements for the clinical investigation of BP monitors. The following subsections outline major guidelines for validation of BP systems from the AAMI/ESH/ISO collaboration statement with additional guidelines from the American College of Cardiology (ACC) and the AHA (Pickering et al., 2005; Stergiou et al., 2018; Whelton et al., 2018).

2.3.1 Measure of Efficacy & Error Analysis

For validated BP systems, an error of $\leq 5 \pm 8$ mmHg or ≤ 10 mmHg within 85% estimated probability is acceptable. These bounds account for the accuracy of current commercially available BP monitors. This tolerable error must be calculated by comparing the individual's average of three BP readings to a reference. At least 85 subjects are required for an AAMI/ESH/ISO validation study. The mean BP difference (test versus reference) and their standard deviations should be applied for systolic and diastolic BP. The results of absolute BP differences within 5, 10, and 15 mmHg should be presented on standardized Bland–Altman scatter plots (Stergiou et al., 2018).

2.3.2 Speed of Cuff Inflation and Deflation

The AHA specifies a minimum deflation rate for cuff deflation of ≥ 2 mmHg per second and suggests a rate between 2 to 3 mmHg per second (Whelton et al., 2017). This standard is specified because faster deflation times can result in underestimation of SBP and overestimation

of DBP. The authors of the standard clarify that devices with linear deflation rates may have improved accuracy over stepwise deflation (a common deflation method for automated systems) (Pickering et al., 2005).

2.3.3 Cuff Size

All validated commercial devices follow the ANSI/AAMI/ISO guidelines for BP cuff size. Standard sizing for BP cuffs is regulated among validated BP devices because cuff size affects BP estimation. Serval studies on cuff size have found that inappropriately sized cuffs can result in incorrect estimation of BP which can impair clinical diagnosis (Lee et al., 2022; Palatini et al., 2020; Palatini & Asmar, 2018). Significantly, this creates issues with universal or standard size cuffs. To mitigate this issue, the standards organizations publish guidelines for selecting appropriately sized cuffs based on arm circumference:

Table 2-2. Selection criteria for BP cuff size for measurement of BP in adults

Arm Circumference	Standard Cuff Size	Bladder Dimensions (W x L)
22-26 cm	Small Adult	12 x 22 cm
27-34 cm	Adult	16 x 30 cm
35-44 cm	Large Adult	16 x 36 cm
42-52 cm	Adult Thigh	16 x 42 cm

The standards on cuff size specify that the ideal BP bladder should have a length that is 80% of arm circumference and a width that is 40% of arm circumference (length: width ratio of 2:1) (Pickering et al., 2005). Inappropriate cuff selection can cause over- or under-cuffing, a phenomenon that results in underestimation or overestimation of BP, respectively. Inaccurate results contribute to both missed diagnosis and misdiagnosis of hypertension (Whelton et al., 2018). For validation of devices with multiple cuff sizes the ANSI/AAMI/ISO standard requires

a minimum number of test subjects (dependent on the number of cuffs assessed), requirements for the distribution of arm circumference sizes, and a detailed description of the reference cuff (Stergiou et al., 2018).

2.4 Mathematical Modeling of Blood Pressure

There are three common empirically inspired algorithms used to estimate BP from the oscillations in cuff pressure. These algorithms are derived from mathematical modeling of the oscillometric waveform (OMW) (Chandrasekhar et al., 2019; Chen et al., 2009). The OMW is obtained from the oscillations in cuff pressure, either by applying a high pass filter to the deflation curve, or by subtracting a baseline from deflation curve. The OMW can be analyzed independently, but it is frequently reduced for simplified analysis. The simplified OMW is represented by an oscillometric waveform envelope (OMWE) which identifies the maximum amplitudes of the pulses without regard for their individual shape (Figure 2-3. Isolation of the OMW and OMWE from the deflation curve.). The OMWE can be fit to the OMW using multiple functions, but it is typically fit by a high order polynomial function, cubic or linear peak-to-peak interpolation, or by a Gaussian function.

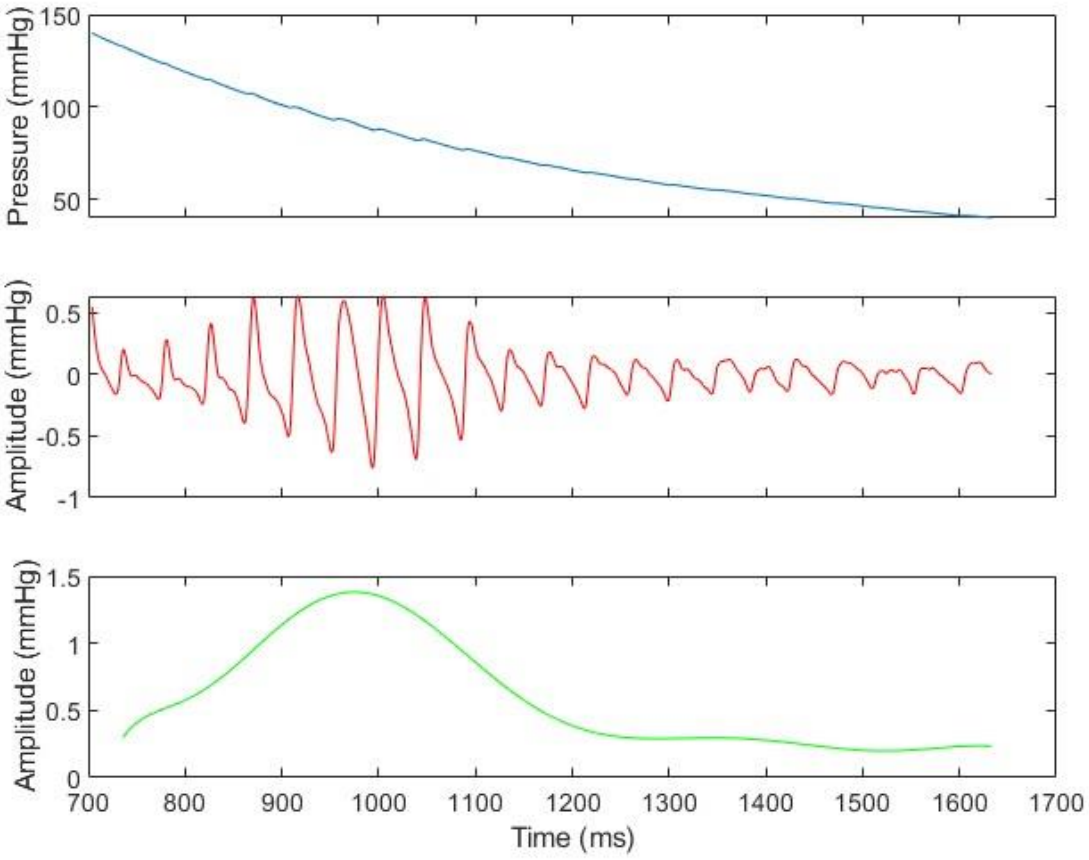

Figure 2-3. Isolation of the OMW and OMWE from the deflation curve. The Deflation curve is represented in blue, small oscillations seen on the curve are heartbeats. The OMW is in red, and the OMWE is in green. The OMW was obtained with a high pass Butterworth filter and the OMWE was obtained by fitting the upper and lower curves of the OMW by cubic interpolation, and then subtracting the lower curve from the upper curve.

Estimation of BP using the OMW or OMWE relies on three assumptions:

1. The artery is purely elastic. This can be modeled as a sigmoidal relationship between blood volume and transmural pressure.
2. The tissue around the artery is incompressible.
3. The relationship between the cuff pressure and air volume is static and linear. They can be related by a constant equal to the reciprocal of the compliance of the cuff, which establishes that the peak-to-peak amplitude of the cuff oscillations are

proportional to the peak-to-peak amplitude of the arterial blood volume oscillations.

With these assumptions, the pressure in the cuff can be mathematically modeled as:

$$\Delta O = kf(P_s - P_e) - kf(P_d - P_e) \quad (1)$$

Where ΔO is proportional to the OMWE, k is the reciprocal of cuff compliance and P_s, P_d, and P_e refer to the SBP, DBP, and the pressure in the cuff. The variable f denotes the function for the relationship between transmural pressure and blood volume (Chandrasekhar et al., 2019).

2.4.1 Maximum Amplitude Algorithm

The maximum amplitude algorithm (MAA) determines mean arterial pressure (MAP) as ratios of the SBP and DBP. The MAP corresponds with the maximum amplitude on the OMWE (Figure 2-4) (Baker et al., 1997).

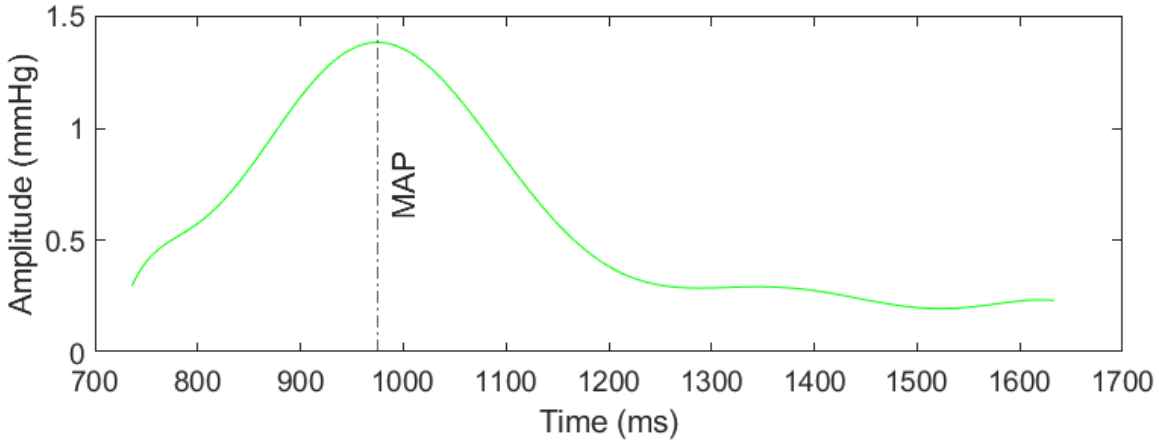

Figure 2-4. Location of the MAP on the OMWE.

The maximum is caused by the buckling of the artery under pressure, which occurs when the artery is most compliant. The MAP is related to this point of compliance (near zero transmural pressure), and therefore is related to the maximum amplitude on the OMWE (Drzewiecki et al., 1994; Mauck et al., 1980). The MAP and its relationship to SBP and DBP have been evaluated in several studies and three characteristic equations are frequently utilized:

$$MAP = \frac{1}{3}SBP + \frac{2}{3}DBP \quad (2)$$

$$= DBP + \frac{1}{3}(SBP - DBP) \quad (3)$$

$$MAP = \frac{\alpha}{\alpha + \beta}SBP + \frac{\beta}{\alpha + \beta}DBP \quad (4)$$

At rest, approximately one third of the cardiac cycle is spent in systole and the other two thirds in diastole. The first MAA algorithm is a standard formula that reflects these periods in the cardiac cycle (Sainas et al., 2016). The fixed-ratio MAA can be modified for patient-specific scenarios by substituting the fixed ratios for α and β which represent arterial compliance curve widths over negative and positive transmural pressures, respectively (Chandrasekhar et al., 2019).

2.4.2 Maximum Slopes/Derivative Algorithm

The maximum slopes algorithm (MSA) estimates SBP and DBP from the slopes of the OMWE (Figure 2-5). The SBP is estimated as the maximum slope on the rising curve to the

MAP and the DBP is estimated as the minimum slope on the falling curve from the MAP (Chandrasekhar et al., 2019; Chen et al., 2009; Forouzanfar et al., 2015).

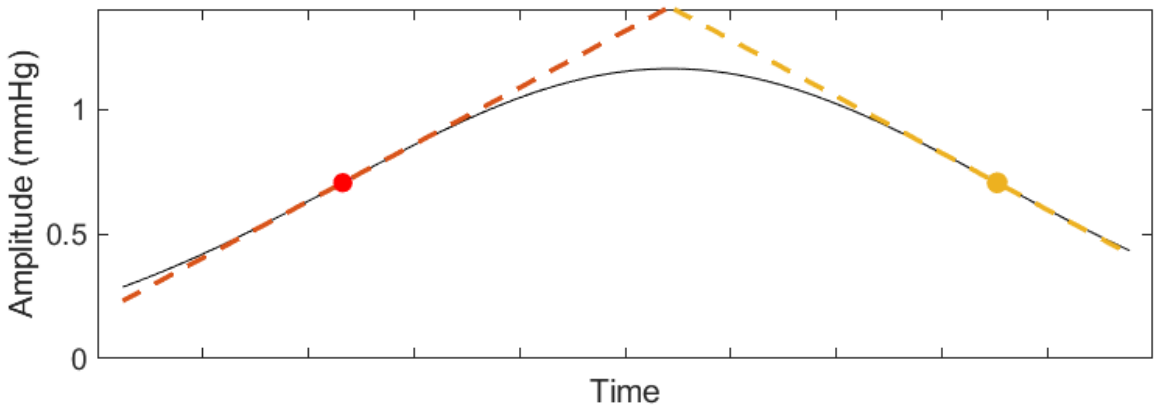

Figure 2-5. The location of the maximum and minimum slopes on the Gaussian fitted OMWE.

These points can be located on the OMWE because of the relationship between BP and arterial compliance. When BP approaches the SBP, the artery is less compliant and fewer oscillations can be detected. The inverse compliance occurs for DBP; when BP is low the artery is more compliant and the cuff is less sensitive to volume change (Drzewiecki et al., 1994). The results of the MSA can be accurately predicted with sufficient noise suppression, but the estimation of SBP and DBP can still vary based on the fitting of the OMWE. This model is particularly advantageous if a high-quality signal can be obtained because there are no empirical coefficients (Forouzanfar et al., 2015). Evaluation of the MSA demonstrates that a Gaussian-fit OMWE may be more appropriate for MSA calculation (Alvarez, 2022).

2.4.3 Maximum Amplitude Ratio/Fixed-ratio Algorithm

The exact algorithms used to calculate BP from automated devices are proprietary to the manufacturer, but it is believed most commercial devices use the fixed-ratio algorithm (MAR) or

some variation of it (Raamat et al., 2013). (Likely, the MAR is augmented with private collections of BP data.) The MAR estimates SBP and DBP as fixed ratios of the MAP.

These fixed ratios were determined empirically and are based on population averages (Drzewiecki et al., 1994; Geddes et al., 1982):

$$\frac{SBP}{MAP} = 0.55 \tag{5}$$

$$\frac{DBP}{MAP} = 0.85 \tag{6}$$

On the OMWE, the SBP is found on the rising curve of the MAP and the DBP is found on the falling curve. The MAR is shown in (Figure 2-6) with the original deflation curve.

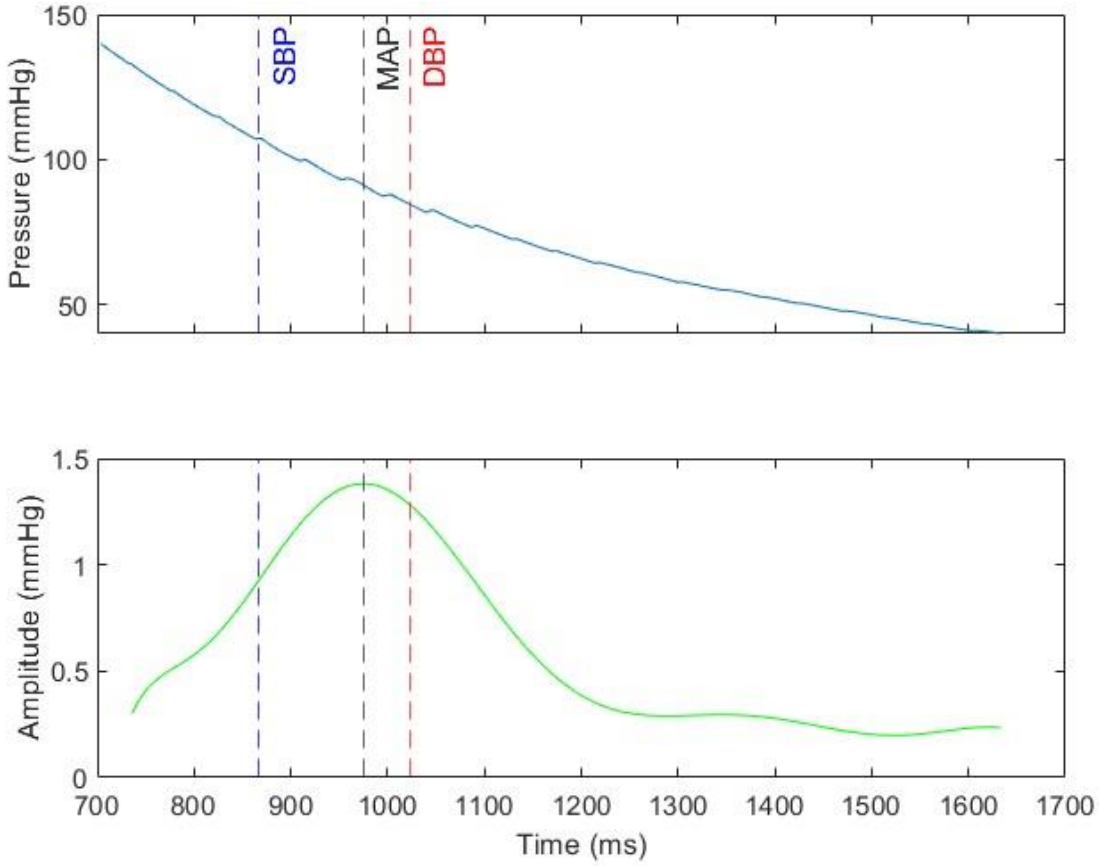

Figure 2-6. The MAR for estimating BP.

The locations for SBP (blue) and DBP (red) are found at $0.55 \times MAP$ and $0.80 \times MAP$, respectively. These points can be traced from the OMWE to the deflation curve, where SBP and DBP are estimated in mmHg. Notably, the location of the SBP and DBP of the OMWE can vary by device.

3 Materials and Methods

Current wearable BP monitors focus on estimating BP via novel techniques, like PPG to analyze pulse transit time. This unprecedented approach for BP monitoring is valuable but critically limited by lack of clinical accuracy. In contrast, the oscillometric method for BP estimation is clinically validated and has been performed for over a century. There are a small number of wearable oscillometric BP monitors that are commercially available, but these systems are bulky and uncomfortable for long-term wear. In this investigation, a thin, low-profile, wearable BP monitoring system was designed to address the obstacles associated with wearable BP monitors.

3.1 System Overview

This project assessed the feasibility of using a small bladder for the estimation of BP with the intention of integration into a wearable device. Wearable integration is proposed via a shirt to create smart, health-oriented apparel. The BP device is comprised of a pressure transducer, analog-to-digital converter (ADC), microcontroller unit (MCU), a valve, a pump, and two 18650 batteries. All electronic components are contained in a small box that can be mounted on the arm, or later, integrated into an apparel item. The device can accommodate multiple sizes of oscillometric bladders; two bladders with widths of 5 cm and 3 cm were designed to assess narrow-cuff estimation.

To estimate BP, the valve and motor in the device are powered. This action closes the valve and turns on the motor. The motor runs to a specified pressure (based on the size of the cuff) to occlude the artery. Once the specified pressure is reached, the device cuts power to the valve and motor. Pressure in the cuff is released from the open valve while the pressure

transducer constantly records the pressure in the cuff. When the pressure in the cuff drops below the DBP value, BP estimation can be computed.

3.2 System Design

A block diagram of the system is presented in Figure 3-1. The system is comprised of five functional blocks that communicate to control cuff inflation and record pressure within the cuff.

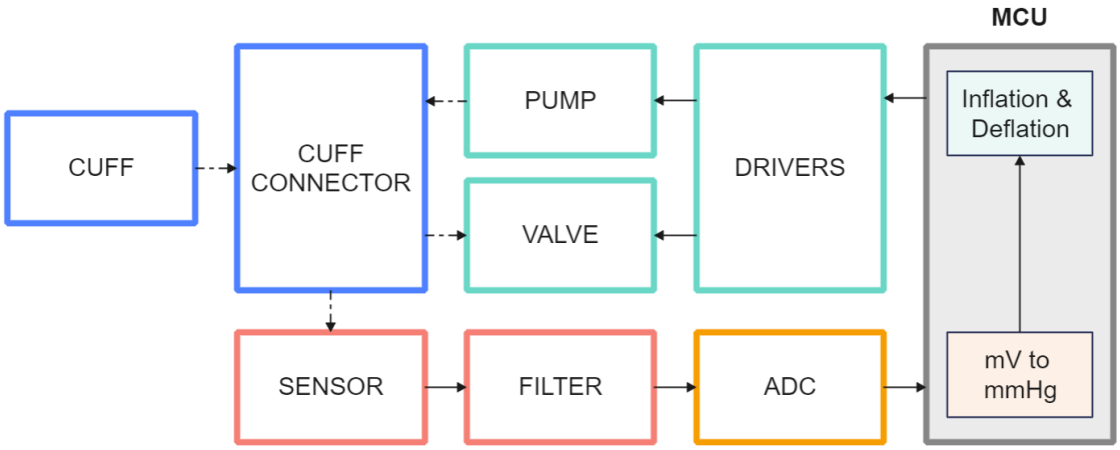

Figure 3-1. Block diagram of the system design. Electrical connections are shown in solid lines, and tube connections are represented by dashed lines.

The physical system is presented in Figure 3-1 and Figure 3-2. The monitoring system contains an electrical box and the ability to connect to multiple wearable BP cuff sizes via the cuff connector. The cuff is shown in the proposed wearable system, embedded in a compressive shirt.

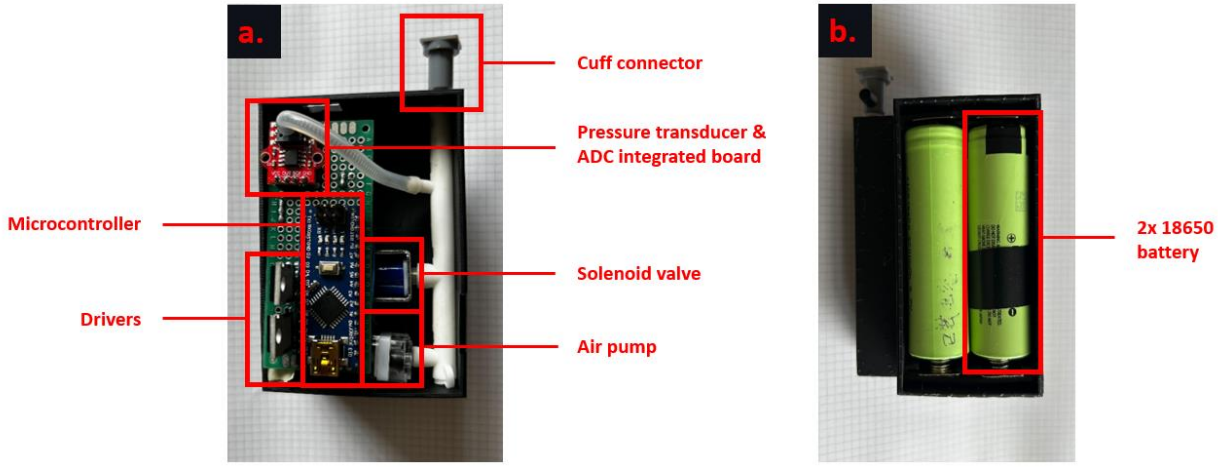

Figure 3-2. Electrical hardware box & components. The front and back of the box are shown: a. Pressure sensing system; b. Batteries.

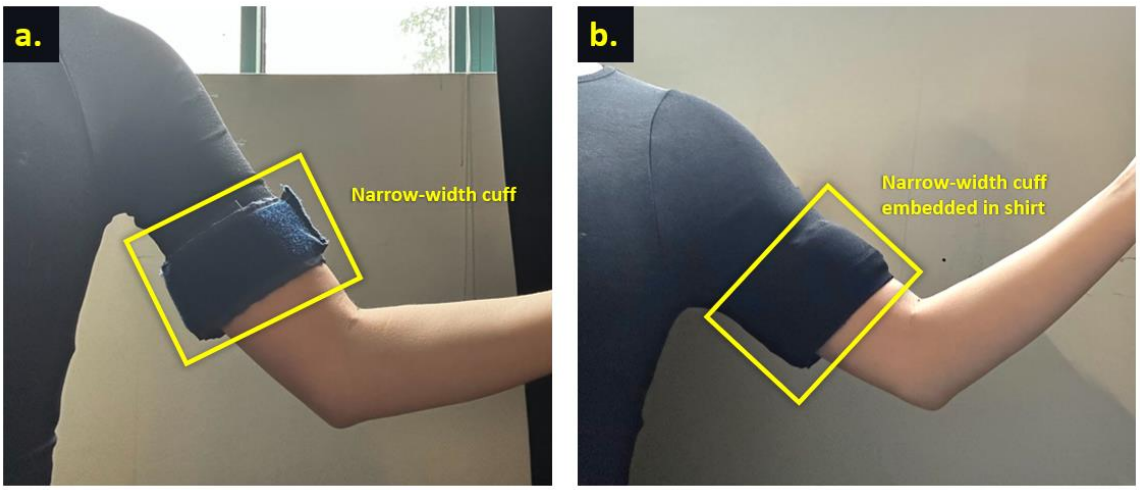

Figure 3-3. Narrow-width cuff positioning. The cuff is shown in two scenarios: a. the cuff is placed on the arm, below the shirt sleeve and level to the right atrium (experimental setup); b. the cuff is shown in the same position, integrated into a compressive shirt (future wearable integration).

3.2.1 Microcontroller Unit

For prototyping purposes, this BP system used an ELEGOO Nano V3.0, which is an MCU based on the Arduino Nano (manufactured by Arduino) and is compatible with the Arduino integrated development environment (IDE) (Arduino, n.d.; Elegoo, n.d.). This MCU

relies on the ATmega328, an 8-bit AVR RISC-based microcontroller manufactured by Microchip (Microchip, n.d.). The ELEGOO Nano V3.0 runs on an operating voltage of 5V, and has a built-in 10-bit ADC, two inter-integrated surface (I2C) ports, four serial peripheral interfacing (SPI) ports, and 6 ports for pulse-width modulation (PWM).

3.2.2 Analog to Digital Converter

The BP sensing module is dependent on an ADC to convert analog pressure readings to digital signal. For higher signal resolution the TM7711, a 24-bit ADC by Titan Micro Electronics was used instead of the built-in ADC on the MCU (Titan Micro Electronics, n.d.). The operating voltage for the ADC is 2.6 to 5.5V and the analog differential input voltage range is ± 10 mV. The TM7711 communicates with the MCU via serial clock and data bin, in a unidirectional SPI-like interface and features an on-chip low noise amplifier with 128 gain. The ADC can be configured for pressure and temperature with fully differential input channels (linearity ± 0.001%) and selectable data output rates of 10 or 40 Hz. The output rate of the ADC is determined by the serial pulses between the ADC and the MCU. These are no existing Arduino libraries specifically for the TM7711, but the library for the HX711 loadcell amplifier (manufactured by Avia Semiconductors) can be adjusted for the TM771 by increasing the number of serial clock pulses (Avia Semiconductor (Xiamen) Ltd., n.d.). The TM7711 is sold as an integrated board with the MSP40-GSF pressure transducer by MEMSensing Microsystems attached (MEMSensing Microsystems, n.d.). The small size of the integrated ADC-transducer board is advantageous for wearable device design.

3.2.3 Pressure Transducer

The MSP40-GSF pressure transducer was used in the system because of its integration with the TM7711, but it is also distributed individually as an electronic blood pressure monitor pressure sensor. The MSP40-GSF runs on an operating voltage of 5V and has a full-scale analog output of 75 mV. The transducer has an ideal sensing range for BP estimate and can read between 0 to 40 kPa, or 0 to 300 mmHg. The output of the sensor is linearly related to the supply voltage and has a maximum non-linearity of 0.3%.

3.2.4 Inflation-Deflation Components

Inflation and deflation of the BP cuff in the system was facilitated by a single-outlet pump and solenoid valve. The pump and valve were retrieved from the Dynarex Upper Arm BP Monitor Reorder #7096 (Dynarex, n.d.). Both components operated on a range of 3 to 6V. The inflation rate of the pump could be controlled via PWM, but the solenoid valve was unsuitable for PWM for controlled deflation. (Rapid opening and closing of the valve can interfere with analog signal and reduce the lifespan of the actuator.) To reduce the rate of deflation, a custom fitting was attached to the end of the valve to limit the translation of the plunger.

3.2.5 Electrical Circuitry

Analog and digital components of the device were separated to reduce electrical noise. A schematic of the circuitry is shown in (Figure 3-4).

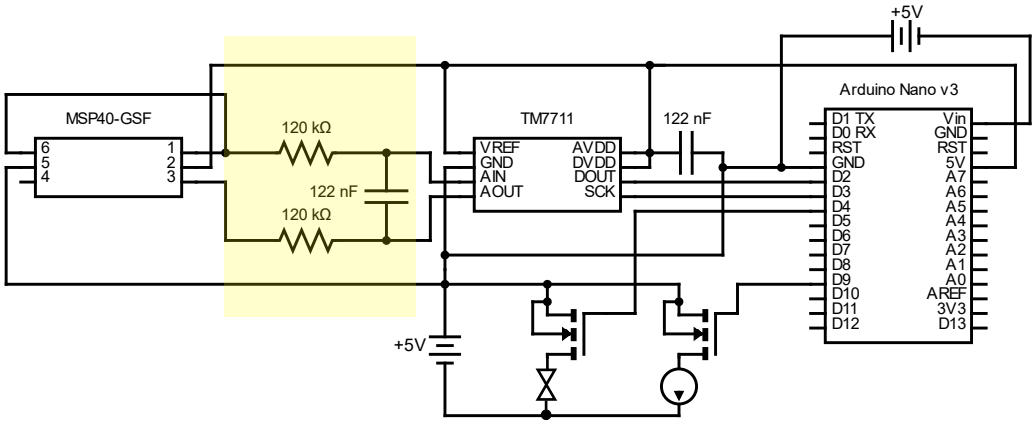

Figure 3-4. Electrical circuit diagram of all components. The modified RC low-pass filter is shown highlighted.

Notably, the TM7711 was distributed with two 1K ohm resistors. These original resistors were removed and replaced with 120 K ohm. The TM7711 can accommodate a maximum input voltage reading of ± 10 mV. The incoming voltage to the ADC with the original 1K ohm resistors was too high for the ADC to interpret, resulting in a max pressure reading of 80 mmHg. Substituting the original resistors with 120K ohm resistors reduced the analog differential output from the transducer, allowing for pressure readings up to 250 mmHg. Substitution of the resistors between the transducer and the ADC changed the parameters of the resistor-capacitor (RC) circuit on the integrated board.

$$f_c = \frac{1}{2\pi RC}$$

$$= \frac{1}{2\pi(120{,}000\ \Omega)(122 \times 10^9\ nF)}$$

$$= 10.87\ Hz \tag{7}$$

The higher ohm resistors reduced the cut off frequency (f_c) of the circuit by over 100-fold, creating a low pass filter with a bandwidth of 0 to 11 Hz. This significantly attenuated noise in the system and promoted a higher quality waveform.

3.2.6 Narrow Width Bladder

Narrow-width BP cuffs were fabricated by sourcing materials from an aneroid adult-thigh sphygmomanometer, manufactured by Dixie EMS (Dixie EMS, n.d.). The bladder from the original sphygmomanometer was removed and then measured for a thin cuff, leaving the tubing intact. Two thin cuffs were created, with two distinct bladder sizes. Bladder widths were chosen at 5-cm and 3-cm (38% and 23% of the original cuff size, respectively). Bladders were cut to smaller widths with a 1.5 cm seam allowance. The length of the bladder was not modified. Each modified bladder was individually sealed with a heat press on the seam allowance. The material of the bladder was protected from direct contact with the heating element by Teflon sheeting. The seams of the narrow-width bladders were pressed for 45 seconds at 385˚F to maintain an airtight seal (Figure 3-5).

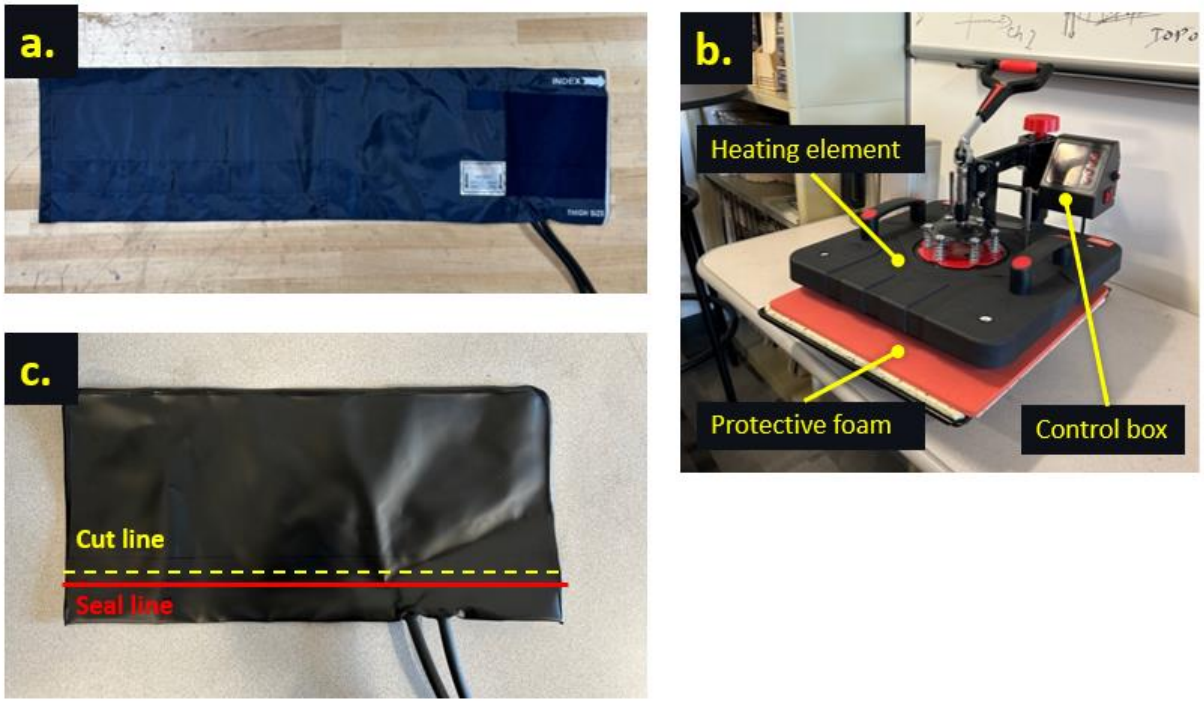

Figure 3-5. Components for the assembly of a narrow-width bladder: a. the original Dixie EMS cuff; b. the heat press; c. the unaltered bladder removed from the Dixie EMS thigh cuff (on the bladder, the dashed line represents where the material was cut, and the area between the dashed and solid line is the seam allowance for a 3-cm cuff).

After modification of the bladder, the rest of the material from the Dixie EMS cuff was repurposed to encase the bladder. The bladder was placed in the repurposed sleeve with 1 cm seam allowance. The seam of the bladder was sewn directly into the fabric cuff to minimize movement of the bladder. The final narrow-width bladders are shown in Figure 3-6.

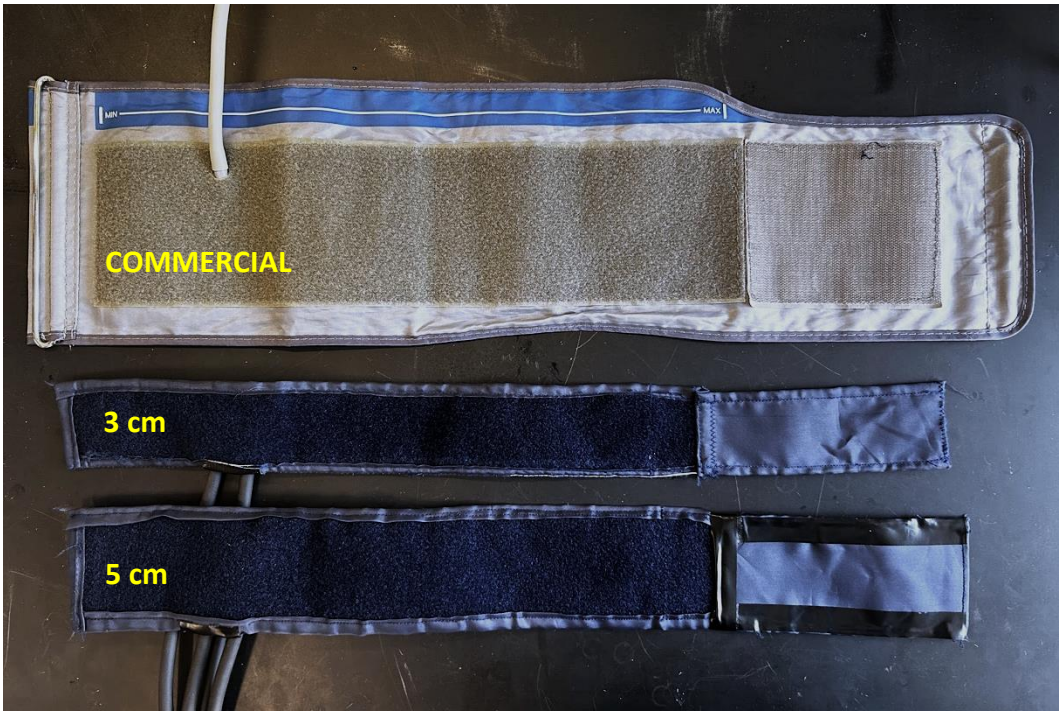

Figure 3-6. Comparison of narrow-width cuffs with commercial cuff. From top to bottom: commercial BP cuff manufactured by Beurer for the BM67 Upper Arm BP Monitor, 3-cm cuff, 5-cm cuff.

3.3 Blood Pressure Measurement

Blood pressure measurement was guided by the universal standards for BP validation (Stergiou et al., 2018). Prior to measuring BP on the subject, the device was calibrated to ensure its accuracy.

3.3.1 Calibration of the Sensor

The sensor was calibrated against an aneroid pressure gauge with a standard ABPM cuff manufactured by Dixie EMS. The voltage reading displayed from serial communication with the ADC was verified with a multimeter:

$$D = \frac{(2^n - 1) \times (V_{AIN})}{V_{REF}} \times g$$

The digital output (D) in the monitor was verified from the reference voltage (V_{REF}), the analog input voltage across the ADC (V_{AIN}), the resolution of the ADC (24-bit) (n), and the built-in gain (g). After the ADC reading was verified, the transducer was connected to the bladder. The bladder was inflated in increments of 20 mmHg and the analog sensor reading and ADC reading were recorded using a multimeter. The relationship between the sensor and pressure was linear ($R^2 = 0.9996$) (Figure 3-7).

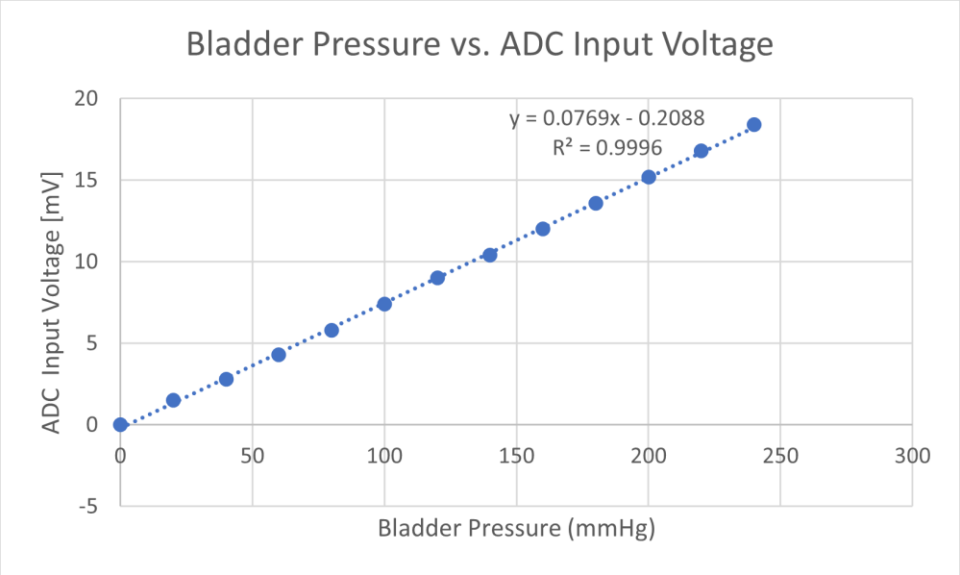

Figure 3-7. Calibration of the BP monitoring system.

3.3.2 Experimental Procedure

The circumference of the subject's left arm was measured and then BP was measured with a same-arm sequential method in the left arm. All measurements were taken with the subject seated with their feet and back supported. Subjects were asked to empty their bladders

before BP measurements were taken and instructed not to talk or move during the testing procedure. All clothing was removed from the site of measurement before the procedure began.

A total of thirteen measurements were taken per subject, with twelve measurements used in data analysis (first measurement discarded) (Table 3-1). For each measurement, the subject was asked to rest their arm on a desktop and then the appropriate cuff was positioned on the upper arm at the level of the right atrium. For reference measurements, the SBP, DBP, and heart rate (HR) were recorded. For measurements on the experimental setup, pressure in the cuff was continuously monitored by the pressure transducer and recorded by the ADC during inflation and deflation of the cuff. Measurements were taken intermittently, with two-minute rest periods between readings.

Table 3-1. Procedure for reference and test device BP measurements in same arm.

Initial BP Measurement		
1.	Take reference BP Measurement	R_0
Validation BP measurements for accuracy evaluation		
2.	Take first reference BP Measurement	R_1
3.	Take first BP measurement on experimental system with commercial cuff	T_{COM1}
4.	Take first BP measurement on experimental system with 5-cm cuff	T_{5CM1}
5.	Take first BP measurement on experimental system with 3-cm cuff	T_{3CM1}
6.	Take second reference BP Measurement	R_2
7.	Take second BP measurement on experimental system with commercial cuff	T_{COM2}
8.	Take second BP measurement on experimental system with 5-cm cuff	T_{5CM2}
9.	Take second BP measurement on experimental system with 3-cm cuff	T_{3CM2}
10.	Take third reference BP Measurement	R_3
11.	Take third BP measurement on experimental system with commercial cuff	T_{COM3}
12.	Take third BP measurement on experimental system with 5-cm cuff	T_{5CM3}
13.	Take third BP measurement on experimental system with 3-cm cuff	T_{3CM3}

Reference BP was estimated using a Beurer BM67. The device features a universal cuff with a 13 cm bladder and Bluetooth-enabled monitoring capability. The Beurer inflates to 160 mmHg and then begins deflation. Inflation parameters for the experimental cuffs differed by cuff

size to ensure occlusion of the artery. For T_{COM}, the cuff was inflated to 160 mmHg. For T_{5CM} and T_{3CM} the cuff was inflated to 220 mmHg.

3.4 Data processing

Data was processed in four segments. First, all the reference data was analyzed for variability. Waveform information was then collected from the experimental data. Multiple algorithms and regression analyses were performed on the waveforms to estimate BP. For overarching analysis, experimental BP estimations were compared to the reference data.

3.4.1 Analysis of Reference Data

Estimations for SBP, DBP, and HR were collected from the reference BP monitor. The MAP of each subject was calculated from the SBP and DBP using the standard ratios in the MAA from Section 2.4.1. The ratio of SBP to MAP and DBP to MAP was computed for each subject. The mean and standard deviation (SD) of all the ratios of SBP to MAP and DBP to MAP were computed for proportional analysis with the experimental data.

3.4.2 Filtering the Deflation Signal

The cuff pressure signal was constantly logged and recorded during inflation and deflation of the cuff. The pressure signal during deflation was isolated for signal filtering and oscillometric analysis. The range of isolated pressure differed between the commercial cuff and the smaller cuffs due to the differences in maximum inflation pressure. Each isolated deflation signal was processed in Matlab with a Butterworth bandpass filter. The filter specified a bandwidth of 0.9 to 3 Hz, with the assumption all heartbeats would fall within this range. This

assumption was based on empirical data on human HR that found the average HR to be between 60 and 300 beats per minute (BPM) during rest and exercise, respectively (Olshansky et al., 2022). Filtration of the deflation pressure resulted in a raw OMW (OMW_1), as seen in Figure 2-3.

A second OMW (OMW_2) was created for the Gaussian enveloping fitting using the raw OMW. To obtain the OMW_2, an envelope was fitted to the lower curve of OMW_1 by piecewise cubic interpolation. This envelope was subtracted from OMW_1 to create an OMW with the baseline of the pressure signal removed (Figure 3-8). (For data collection with larger cuff size, this step could be substituted for fitting a baseline to the deflation curve and subtracting the baseline from the deflation signal. This extra step was taken here because the magnitudes of the oscillations were too small to perform a baseline curve fitting.)

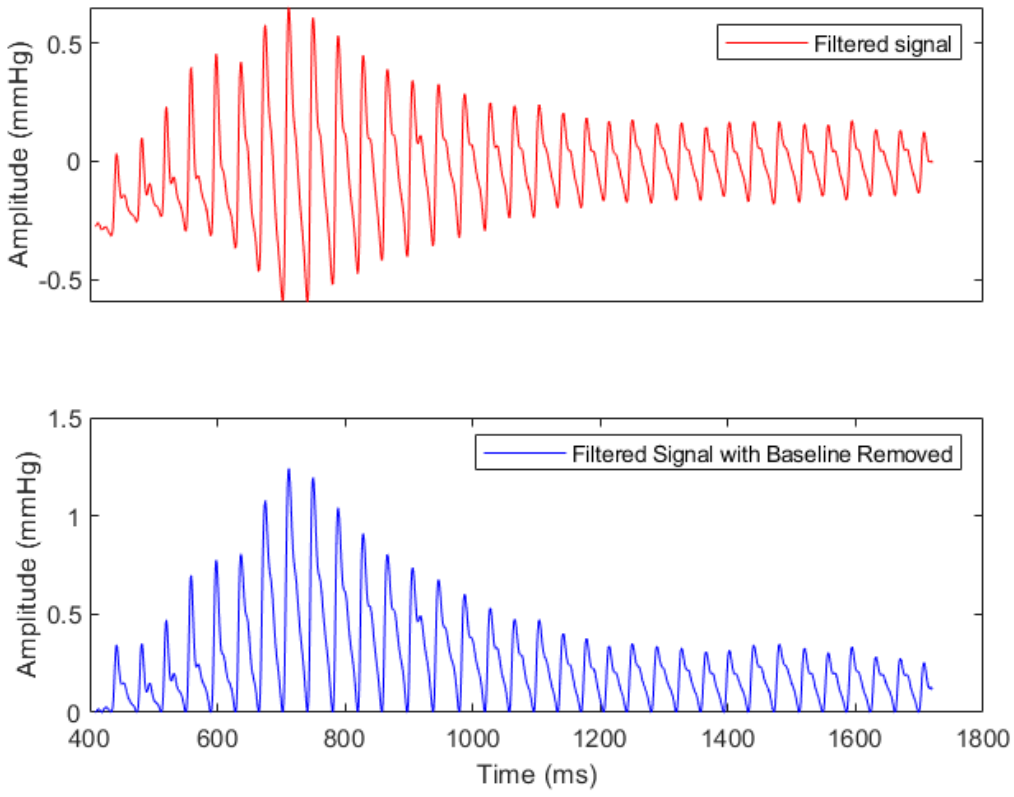

Figure 3-8. Comparison of the raw oscillometric signal and the signal with the baseline removed.

3.4.3 Creation of the Oscillometric Waveform Envelope

An OMWE was obtained for both OMW_1 and OMW_2. For OMW_1, the upper and lower curves of the OMW were fitted with piecewise cubic interpolation envelope. The lower envelope was subtracted from the upper envelope for a rough OMWE. For smoother analysis, a 9^{th} order polynomial was fitted to the rough OMWE to obtain a smooth envelope ($OMWE_1$). For OMW_2, an envelope was fit to the upper curve of the OMWE using spline interpolation with not-a-knot end conditions. The spline-interpolated envelope was fitted with a single Gaussian curve to create a uniform symmetrical envelope ($OMWE_2$). Gaussian fit was specifically performed for the MSA. Small oscillations found in the polynomial fitted OMWE could impact the effectiveness of the MSA algorithm's ability to detect maximum and minimum curves.

3.5 Application of Blood Pressure Algorithms

The MAA, MAR, and MSA discussed in Section 2.4 were all used to analyze the collected data. The MAA was applied to the reference data (discussed above) and the MAR and MSA were applied to the OMWEs.

3.5.1 Implementation of the MAR Algorithm

The MAR algorithm was performed on $OMWE_1$, the polynomial-fit OMWE. This OMWE had a tighter fit to the OMW than $OMWE_2$, and thus it was determined it was more suitable for the MAR algorithm. (Notably, use of the MAR was examined on $OMWE_2$ and an average difference of <5 mmHg was noted between MAP BP estimations from the different OMWEs.) The MAR was used to determine SBP, DBP, and the MAP with the ratios of 0.55 and 0.6 for SBP and DBP, respectively. (These ratios were found to best match the reference device.)

Secondary estimation of SBP and DBP used the MAP derived from the MAR and MAA algorithms to compute SBP and DBP proportional to the SBP and DBP estimated by the reference.

3.5.2 Implementation of the MSA

The MSA was evaluated exclusively on the $OMWE_2$, the Gaussian-fit OMWE. Variation with curve smoothness in $OMWE_1$ affected outputs from the MSA resulting in identification of maximum and minimum slopes at irrelevant points on the waveform. The characteristics of the Gaussian function corrected this issue on $OMWE_2$.

3.6 Calibration of Blood Pressure Estimation

Misalignment between BP estimation with the reference monitor and the experimental setup was expected due to smaller cuff width. This error was calibrated by linearly shifting the BP estimates from the experimental set up. To test the efficacy of the calibration, two-thirds of the data was used for generating the calibration curve. The other third of data was calibrated using the calibration curve. To derive the calibration curve, both the SBP and DBP test estimates were plotted against the reference estimates to determine the degree of error, and a linear regression analysis was performed. The linear function that described the regression line was used to re-compute the experimental BP estimation.

4 Results

4.1 Subjects

A total of 10 subjects participated in this study. A smaller subgroup of 6 subjects was analyzed based on their cuff size (< 30 cm) (Table 4-1). Data related to subjects was discarded if the maximum difference between reference SBP and DBP estimations was > 12 mmHg and > 8 mmHg, respectively (subject #7). Data related to specific cuff size was discarded if issues were detected in the raw OMW signal. This yielded a dataset of 18 reference BP estimations, 18 raw OMWs for the commercial and 5-cm cuffs, and 12 raw OMWs for the 3-cm cuff.

Table 4-1. Reference BP estimation.

Subject #	Arm Circumference (cm)	Sex	Trial #	SBP (mmHg)	DBP (mmHg)	PP (mmHg)	HR (BPM)
1	25	F	1	87	58	29	66
			2	94	64	30	79
			3	92	58	34	68
2	26	M	1	117	72	45	69
			2	117	77	40	68
			3	112	71	41	69
3	25	F	1	97	57	40	79
			2	88	56	32	70
			3	97	53	44	80
4	21	F	1	97	66	31	68
			2	92	62	30	72
			3	90	62	28	71
5	25	F	1	117	77	40	57
			2	119	82	37	77
			3	117	83	34	85
6	28	M	1	110	68	42	58
			2	103	65	38	55
			3	111	68	43	54
7	22	M	1	141	79	62	72
			2	130	78	52	79
			3	123	74	49	77
8	30	M	1	117	82	35	89
			2	119	78	41	90
			3	118	88	30	83

9	37	M	1	138	83	55	64
			2	126	83	43	65
			3	123	81	42	68
10	34	M	1	117	68	49	63
			2	117	62	55	59
			3	121	68	53	55

4.2 Validation of Experimental Device

The experimental device was validated by comparing measurements taken with the commercial reference BP monitor to measurements taken with the experimental device. All measurements for validation were performed with the standard commercial BP cuff. For validation purposes, BP estimates using the MAR, MSA, and reference-proportional MAP were all compared. All measurements fell within the ANSI/AAMI/ISO standards for validated devices outlined in Section 2.3.1. Table 4-2 shows the mean absolute difference between the reference and experimental estimations, the standard deviation between readings, and the limits of agreement (LOA). The LOA reflect all the data that falls within two standard deviations of the absolute mean error, provided that the distribution of data is normal (Figure 4-1).

Table 4-2. Validation of the experimental device.

		Mean Absolute Error (mmHg)	Mean Error ± SD (mmHg)	LOA (mmHg)
MAR	**Total**	5.14	-0.21 ± 5.96	-6.17 to +5.75
	SBP	5.33	-3.36 ± 5.22	-8.58 to +1.87
	DBP	4.95	2.94 ± 4.99	-2.05 to +7.92
MSA	**Total**	4.84	-0.46 ± 6.00	-6.46 to +5.54
	SBP	5.48	-4.19 ± 5.42	-9.61 to +1.22
	DBP	4.20	3.27 ± 3.91	-0.64 to +7.18
MAP	**Total**	4.68	3.28 ± 5.23	-1.94 to +8.51
	SBP	6.22	4.10 ± 6.57	-2.74 to +10.67
	DBP	3.13	2.47 ± 3.42	-0.95 to +5.88

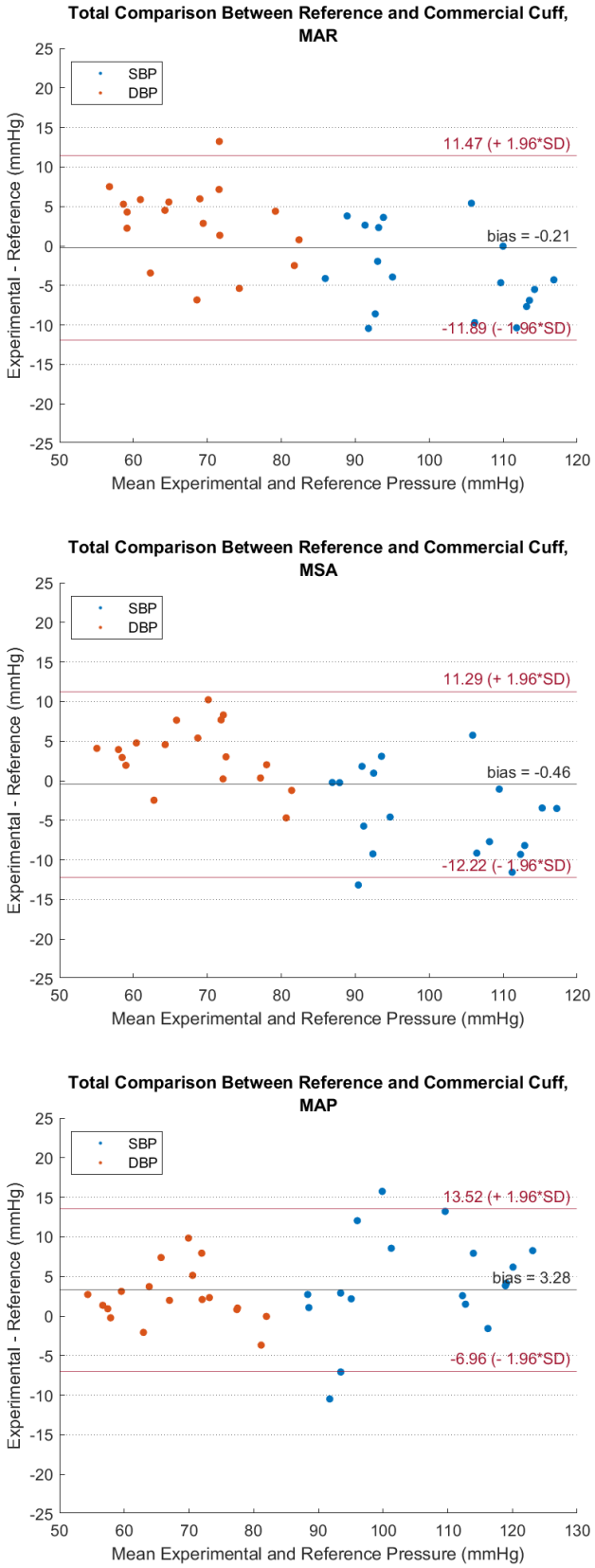

Figure 4-1. Bland-Altman Plots for visualization of the validation of the experimental device.

4.3 Algorithm Estimation

When used for a smaller cuff size, the traditional BP algorithms significantly overestimated BP. As shown in the Bland-Altman plots of Figure 4-2 and Figure 4-3, the mean bias for the 5-cm cuff averaged 13 mmHg higher than the reference value and the mean bias for the 3-cm cuff averaged 31 mmHg higher than the reference value.

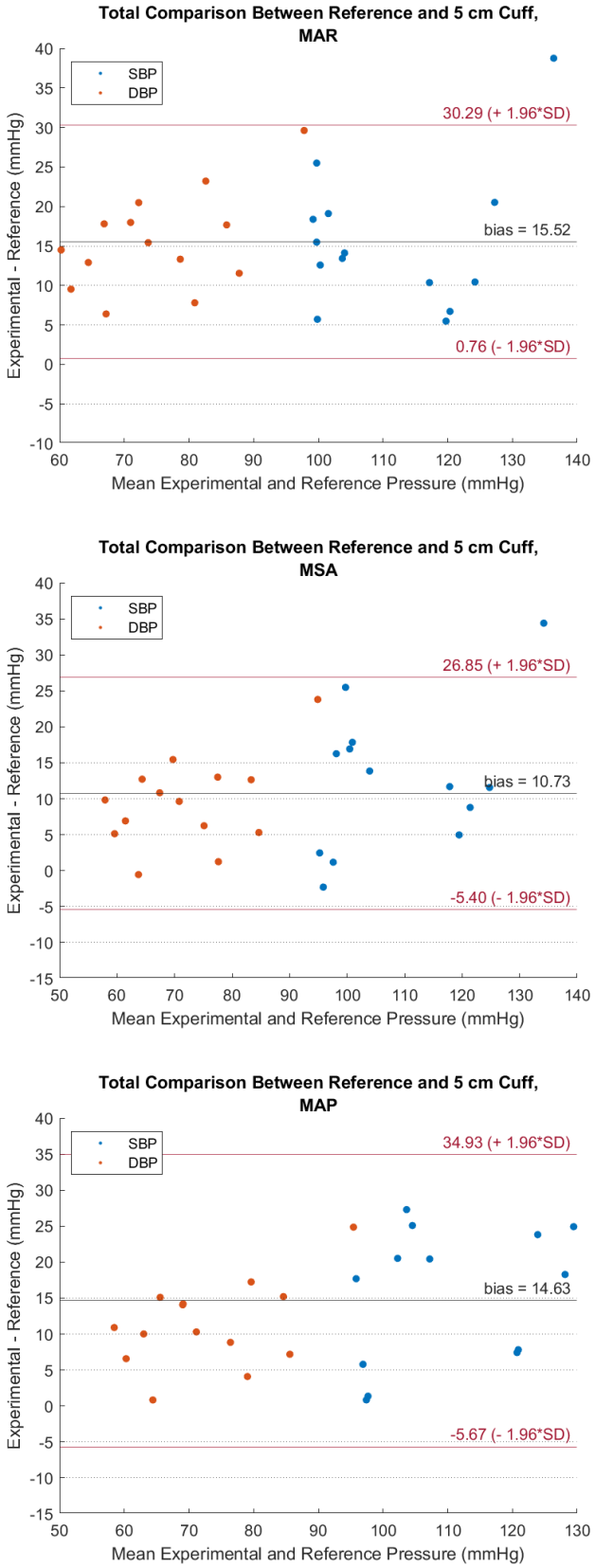

Figure 4-2. Estimation of BP in 5-cm cuff before calibration.

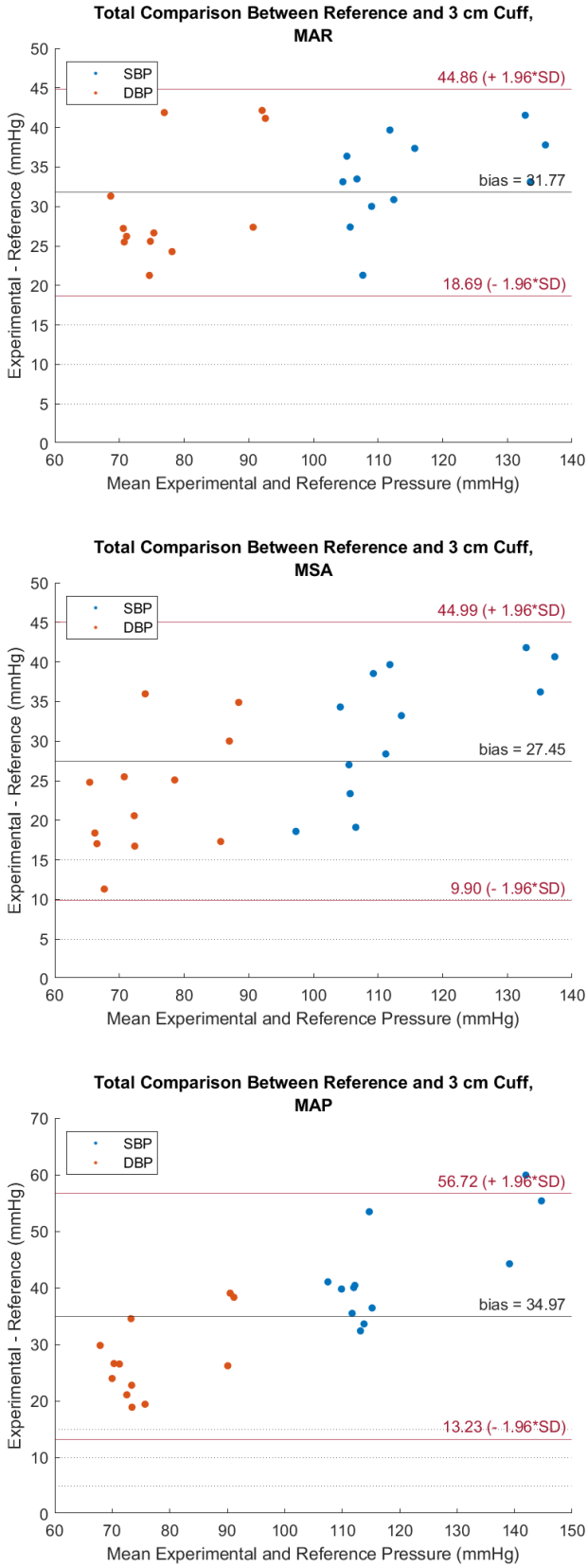

Figure 4-3. Estimation of BP in 3-cm cuff before calibration.

4.4 Calibration of BP Algorithm

The calibration curve of the BP algorithm was calculated using a linear regression analysis. A comparison of the SBP and DBP obtained using small cuffs and the reference commercial BP monitor revealed a linear relationship between BP estimations. Linear regression was performed individually for the SBP and DBP estimations of each algorithm (Figure 4-4 and Figure 4-5).

The agreement between the reference and the calibrated estimations was visualized in multiple Bland-Altman plots. Figure 4-6 and Figure 4-7 depict the calibrated BP estimations for the 3-cm and 5-cm cuffs and describe the overall mean difference (bias) ± the standard. These findings are consolidated in Table 4-3.

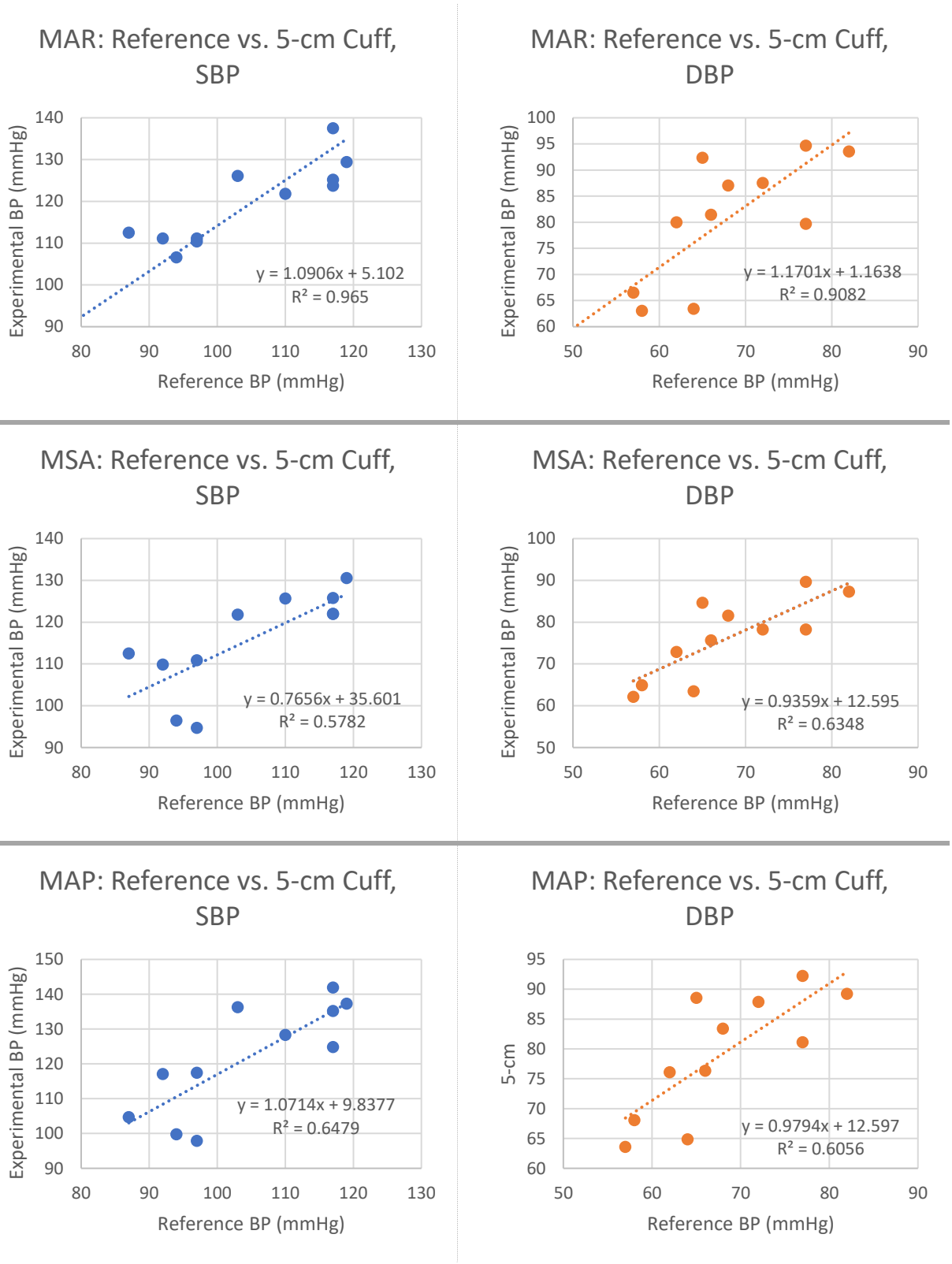

Figure 4-4. Calibration with linear regression for 5-cm cuff.

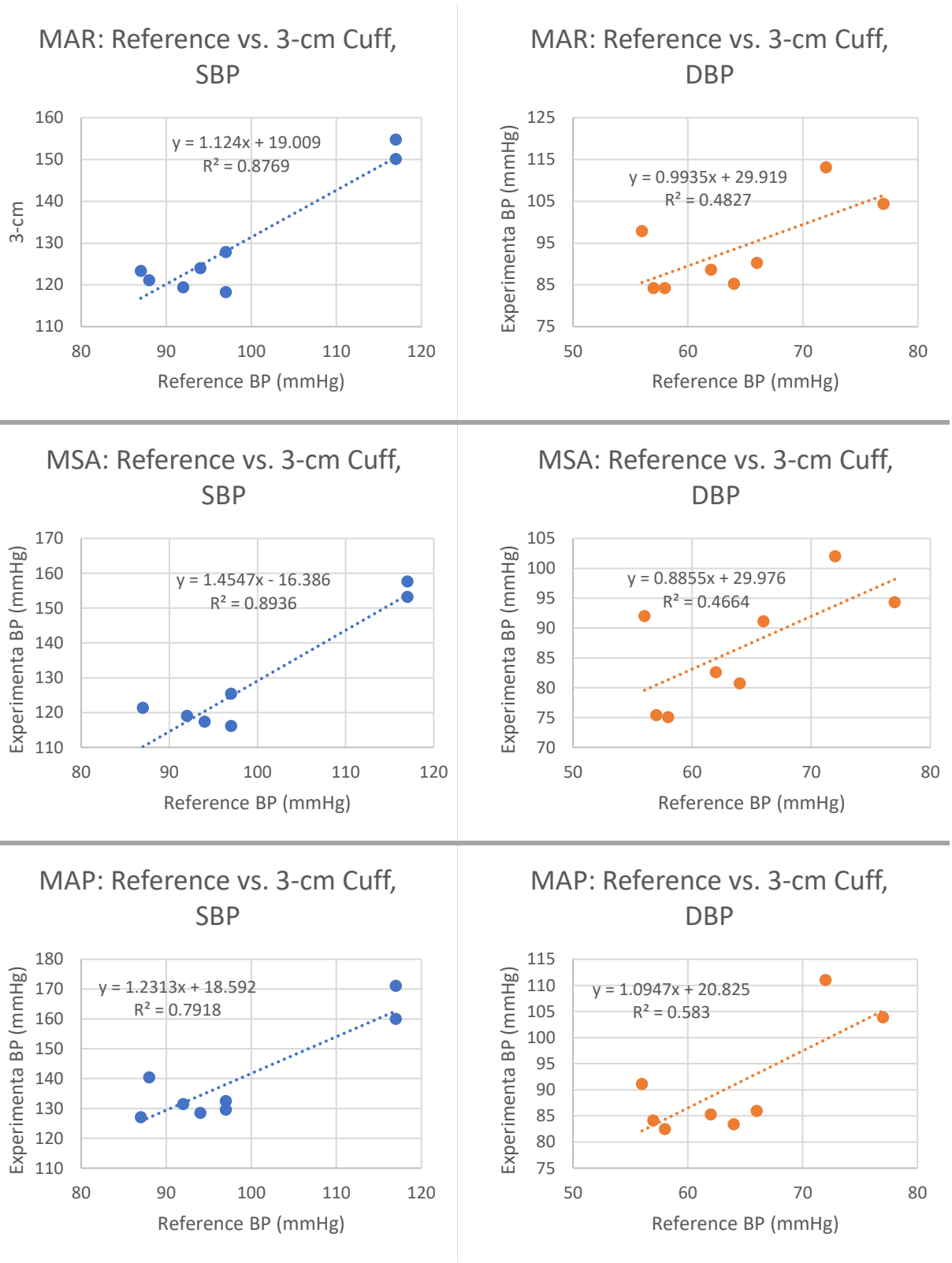

Figure 4-5. Calibration with linear regression for 3-cm cuff.

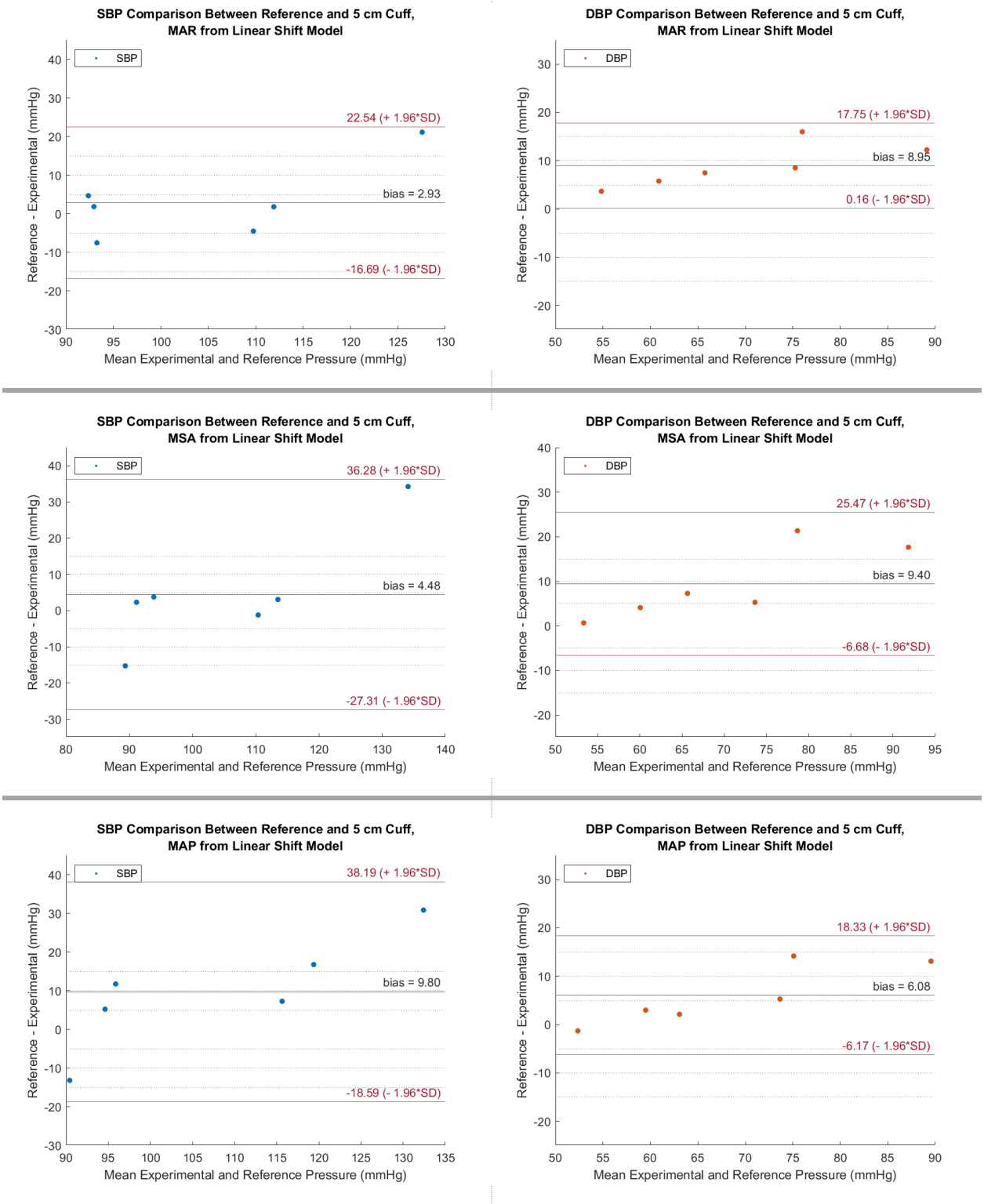

Figure 4-6. Agreement between reference and 5-cm cuff after calibration.

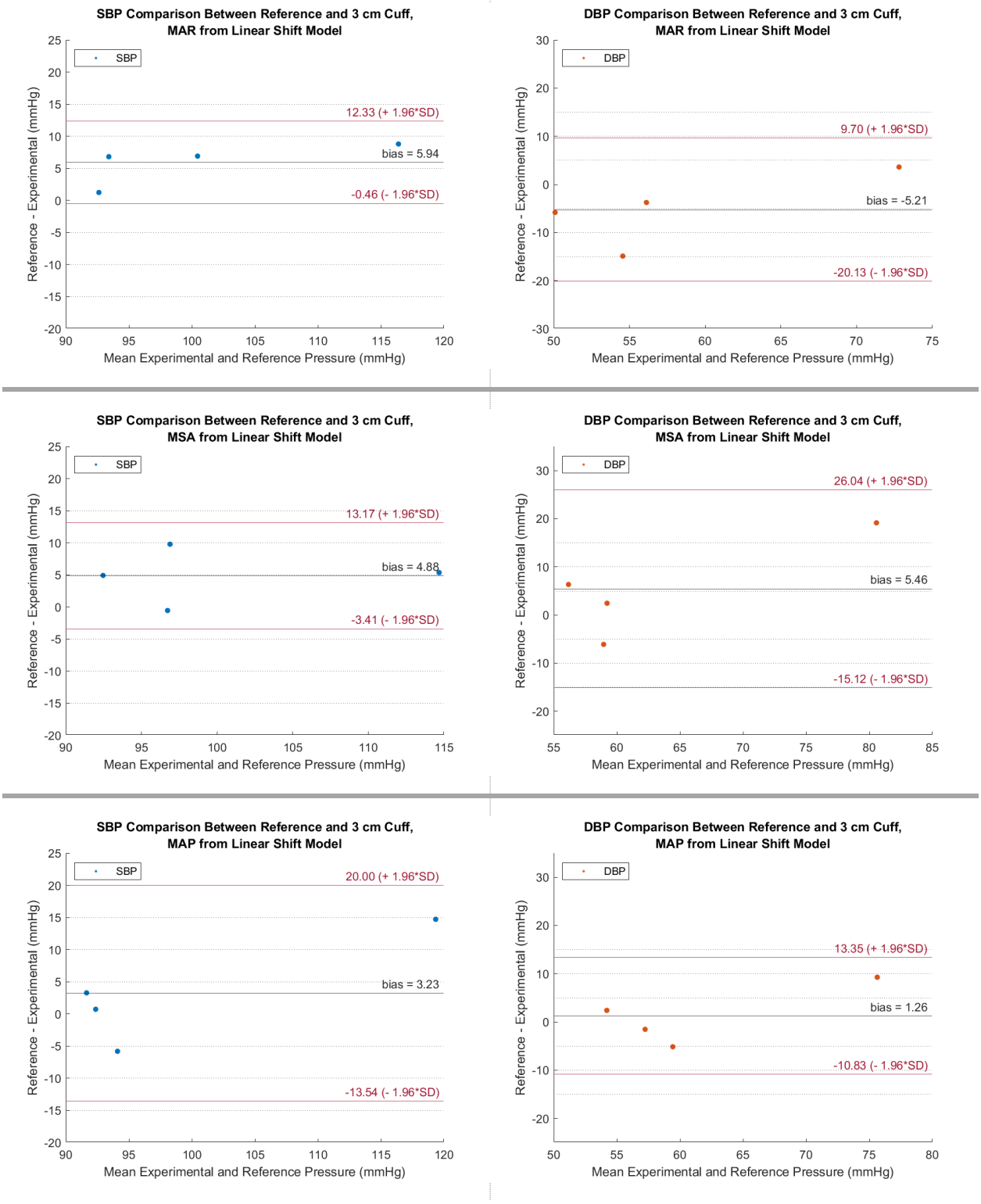

Figure 4-7. Agreement between reference and 3-cm cuff after calibration.

Table 4-3. Agreement between BP estimations from reference monitor and narrow-width cuffs.

			Mean Absolute Error (mmHg)	Mean Error ± SD (mmHg)	LOA (mmHg)	Estimated Probability
5-cm Cuff	MAR	Total	7.9	5.94 ± 8.04	-2.10 to +13.98	
		SBP	6.2	2.93 ± 10.01	-7.08 to +12.93	0.83
		DBP	8.95	8.95 ± 4.49	+4.47 to +13.44	0.67
	MSA	Total	9.68	6.94 ± 12.52	-5.58 to +19.46	
		SBP	9.97	4.48 ± 16.22	-11.74 to +20.71	0.67
		DBP	9.40	9.40 ± 8.20	+1.20 to +17.60	0.67
	MAP	Total	10.34	7.94 ± 10.81	-2.87 to +18.75	
		SBP	14.18	9.80 ± 14.48	-4.69 to +24.28	0.33
		DBP	6.51	6.08 ± 6.25	-0.17 to +12.33	0.67
3-cm Cuff	MAR	Total	6.48	0.36 ± 8.06	-7.70 to +8.42	
		SBP	5.94	5.94 ± 3.26	+2.68 to +9.20	1.00
		DBP	7.02	-5.21 ± 7.61	-12.82 to +2.40	0.75
	MSA	Total	6.83	5.17 ± 7.42	-2.25 to +12.59	
		SBP	5.15	4.88 ± 4.23	+0.65 to +9.11	1.00
		DBP	8.51	5.46 ± 10.50	-5.04 to +15.96	0.75
	MAP	Total	5.36	2.24 ± 6.98	-4.47 to +9.23	
		SBP	6.13	3.23 ± 8.55	-5.33 to +11.78	0.75
		DBP	4.58	1.26 ± 6.17	-4.91 to +7.43	1.00

4.5 Comparison of Deflation Times

The deflation times of the reference BP monitor and the experimental device were compared to assess the differences in speed of deflation. The deflation time for the reference BP was approximated by assuming a controlled deflation rate of -2.5 mmHg/s between 160 mmHg to 45 mmHg, and then fast deflation of 3 seconds after 45 mmHg was reached. Comparison of the deflation times is shown in Table 4-4.

Table 4-4. Comparison of deflation times.

	Reference BP Monitor	Experimental Device with Standard Cuff	Experimental Device with 5-cm Cuff	Experimental Device with 3-cm Cuff
Mean Deflation Time ± S (s)	~ 50	42.78 ± 25.24	20.09 ± 10.10	25.05 ± 10.74

5 Discussion

A subgroup of six subjects, who were selected for similar bicep circumference size (< 30 cm), were further evaluated in this investigation. The average bicep circumference was 25 ± 2.14 cm, the average reference SBP was 103.17 ± 11.67 mmHg, and the average reference DBP was 66.61 ± 8.96 mmHg. These intake measurements were used for comparison and validation of the experimental BP monitoring system in this study.

The validation of the experimental system required the mean absolute difference between the reference and experimental devices to be ≤ 5 ± 8 mmHg. Three algorithms were used to estimate BP with the experimental device (MAR, MSA, proportional MAP) and their agreement with the reference monitor is shown in Table 4-2. All algorithms met the validation criteria, meaning the experimental BP estimation was within acceptable range of the reference BP estimation. All algorithms were characterized by near zero bias and narrow LOA for the total BP reading. Greater LOA for SBP than DBP were observed in all algorithm estimations which can be explained by higher fluctuations in SBP than DBP. The narrow LOAs and the validation of the experimental system with the standard commercial BP cuff supported subsequent BP estimation with the narrow-width cuffs.

Overestimation of BP was observed in the narrow-width cuffs before calibration. This phenomenon is well-documented, but little literature exists on the cause of overestimation — there are no known mechanistic studies that specifically evaluate cuff size. This study theorizes that the overestimation of BP is caused by poor circumferential distribution of pressure in the bladder compared to larger bladder size. This theory supports the observed overestimation: overestimation was higher in the 3-cm cuff than in the 5-cm cuff. In the 5-cm cuff the mean error was 14 mmHg above the reference estimation, and in the 3-cm cuff the mean error was 31

mmHg above the reference estimation. Bland-Altman plot visualization for BP validation requires reference lines to be drawn at -15, -10, -5, +5, +10, +15 on the y-axis (difference between reference and experimental estimation). Roughly all data should fall within these bounds. For the uncalibrated narrow-width cuffs, the BP estimation was significantly higher than these bounds (Figure 4-2 and Figure 4-3).

Calibration was performed to reduce the overestimation produced by the narrow-width cuffs. Calibration curves were obtained by linear regression. Linear regression was performed separately for SBP and DBP because of the difference in MAR ratios for the SBP and DBP values. A high correlation ($R^2 \geq 0.85$) was observed when simultaneous linear regression was performed on SBP and DBP, but separate regression analysis provided better individual DBP and SBP results. For the 5-cm cuff, the MAR estimation had the strongest calibration curve ($R^2 > 0.90$) for both SBP and DBP (Figure 4-4). For the 3-cm cuff, all algorithms had a similar strength, but regression was strongest for SBP estimation (Figure 4-5).

Calibration curves were calculated with two thirds of the data, and then validated the other third of collected data. Following calibration, overestimation of BP was greatly reduced. For the MAR and MSA algorithms, the mean absolute error fell within the ANSI/AAMI/ISO tolerable error of ≤ 10 mmHg, but the estimated probability was below 85% for most estimations (Table 4-3). The inconsistency predicted by the estimated probability is attributed to the small sample size of the study: if the BP estimation for one subject was outside the tolerable error range, the estimated probability crashed. Improvement of the agreement between the reference monitor and the calibrated narrow-width cuff estimations requires a higher sample size. Observation of the agreement between the reference monitor and the data used for the linear regression calibration (i.e., training data exclusive of validation data) reveals BP estimations

were within 1-2 mmHg of the ANSI/AAMI/ISO standard. This finding indicates that agreement should be acceptable with a larger sample size. If there were a larger disagreement with the training data, the linear regression would be too unpredictable to justify use as a calibration curve. The current level of agreement between systems is promising, but it indicates a need for a study with a larger sample size.

Comparison of deflation times was also assessed in addition to calibration effectiveness. Deflation times were recorded on the experimental setup and approximated for the reference BP monitor. The deflation time for the reference BP monitor was approximately 50 seconds. The deflation times for the 5-cm cuff and 3-cm cuff were 20.09 ± 10.10 and 25.05 ± 10.74, respectively. Notably, the 5-cm cuff had a faster average deflation time than the 3-cm cuff. Because a solenoid valve was used instead of a proportional valve, it is believed the higher air volume in the 5-cm cuff caused faster initial deflation than the 3-cm cuff. The standard deviation between average deflation times for the narrow-width cuffs is noticeably high and could be improved by use of a proportional valve in future design iterations. (Controlled deflation via PWM was not achievable with the solenoid valve.) Compared to the reference BP monitor, average deflation time for the narrow-width cuff was between 15 to 25 seconds faster than for the standard commercial cuff. Overall faster inflation and deflation times were attributed to the lower air volume in the narrow-width cuffs.

These results confirm that a valid experimental BP system was established for use in this study. Without sample-specific calibration, this system produced tolerable BP estimations with a standard commercial cuff but overestimated BP with narrow-width cuffs. With calibration, the system was able to significantly reduce the overestimation of BP with narrow-width cuffs to within 1-2 mmHg range of ANSI/AAMI/ISO tolerance. A weak sample size was analyzed in this

study, but results are promising. These initial findings support the potential for stronger calibration curve generation based on the inclusion of a greater sample size. Future investigation of this topic may demonstrate that tolerable readings with a narrow cuff are achievable.

The initial findings reported here suggest that BP overestimation with narrow-width cuffs can be calibrated to produce normal BP estimations. This substantiates a novel technique for BP estimation using a narrow-width cuff. Narrow-width BP cuffs provide the advantages of unobtrusiveness (improves patient comfort) and faster artery recovery following occlusion. These advantages enable more frequent BP monitoring (faster recovery time) and faster response times. The faster deflation time permits quicker BP estimation and therefore quicker response time to serious changes in BP. This could culminate in a device that is an unobtrusive wearable form factor and allows for near-continuous readings.

6 Conclusion

Blood pressure measurement is a critical component of in-hospital care, and an important ambulatory health metric. The study of BP and associated measuring devices is extensive, and recent trends in BP monitoring focus on non-invasive cuffless techniques for BP estimation. Cuffless techniques for BP estimation have struggled to produce clinically acceptable BP estimations and require frequent cuff-based calibration. Creation of a wearable cuff-based BP technology has the potential to provide clinically acceptable BP results without the need for frequent cuff-based calibration. Moreover, this type of device could be used to further research cuffless technologies by providing an easy mode for cuff-based calibration.

This thesis investigated the potential for narrow, low-profile BP cuffs for wearable upper arm oscillometry. Key contributions included:

a) Development of a BP monitoring system. A BP monitoring system was designed and produced using low-cost, lightweight materials. Blood pressure estimations from this experimental device consistently fell within 5 ± 8 mmHg of the reference BP monitor.
b) Design and fabrication of two narrow-width cuffs with bladder widths of 5-cm and 3-cm. Two narrow-width cuffs were designed specifically for this study and were created using standard biocompatible BP cuff materials.
c) New experimental procedures to address overestimation of BP with narrow-width cuffs. A new calibration algorithm was developed and implemented. Calibration demonstrated significant reduction in overestimation of BP.
d) Faster BP collection with narrow-width cuffs. This allows for increased response time to changes in BP and is potentially less damaging to the vessel.

The results of this study indicate that accurate BP estimation with a narrow-width cuff is feasible using multiple BP algorithms. Overestimation of BP was observed using the traditional BP estimation algorithms, but a significant reduction in error was introduced with the implementation of the calibration algorithm. The readings provided by the narrow-width cuffs fell near acceptable limits of tolerable error, following the universal non-invasive BP protocol discussed in Section 2.3. These preliminary results promote the continued study of narrow-width blood pressure cuffs, with incorporation of a correction algorithm.

7 Future Work

Mass General Hospital is in the process of filing a patent application related to this work. The preliminary results from this study are promising, but validation of the methods proposed in this paper require isolation of different parameters known to affect BP: body mass index, bicep

circumference, hypo/hypertension, age, gender, etc. Future work should examine the repeatability of these methods with these different parameters. If a significant database is collected, this research should extend to a machine learning model. The complexity of a machine learning algorithm would surpass the capacity of the linear regression and allow for more accurate and reliable BP estimations based on specific user-input parameters. If reliably accurate BP estimation can be produced from these improvements, the objective is to integrate this device into wearable “smart” apparel.

8 Bibliography

Alvarez, M. A. (2022). *Study of Physics and Mathematics Principles of Cuff-Based Blood Pressure Measurement Methods* [Doctor of Philosophy]. University of Alberta.

Arduino. (n.d.). *Arduino Nano*. Retrieved August 3, 2023, from https://store.arduino.cc/products/arduino-nano.

Avia Semiconductor (Xiamen) Ltd. (n.d.). *HX711*. Retrieved August 3, 2023, from http://en.aviaic.com/detail/730856.html.

Babadag, K., & Zaybak, A. (2021). Comparing Intra-Arterial, Auscultatory, and Oscillometric Measurement Methods for Arterial Blood Pressure. *Florence Nightingale Journal of Nursing*, *29*(2), 194–202. https://doi.org/10.5152/FNJN.2021.19103

Baker, P. D., Westenskow, D. R., & Kück, K. (1997). Theoretical analysis of non-invasive oscillometric maximum amplitude algorithm for estimating mean blood pressure. *Medical and Biological Engineering and Computing*, *35*(3). https://doi.org/10.1007/bf02530049

Barral, J.-P., & Croibier, A. (2011). Circulatory physiology. In *Visceral Vascular Manipulations* (pp. 27–45). Elsevier. https://doi.org/10.1016/B978-0-7020-4351-2.00002-8

Berger, A. (2001). How does it work? Oscillatory blood pressure monitoring devices. *British Medical Journal*, *323*(7318). https://doi.org/10.1136/bmj.323.7318.919

Campbell, M., & Pillarisetty, L. S. (2019). Physiology, Korotkoff Sound. In *StatPearls*.

Chandrasekhar, A., Yavarimanesh, M., Hahn, J. O., Sung, S. H., Chen, C. H., Cheng, H. M., & Mukkamala, R. (2019). Formulas to Explain Popular Oscillometric Blood Pressure Estimation Algorithms. *Frontiers in Physiology*, *10*. https://doi.org/10.3389/fphys.2019.01415

Chen, S., Groza, V. Z., Bolic, M., & Dajani, H. R. (2009). Assessment of algorithms for oscillometric blood pressure measurement. *2009 IEEE Intrumentation and Measurement Technology Conference, I2MTC 2009*. https://doi.org/10.1109/IMTC.2009.5168742

Chobanian, A. V., Bakris, G. L., Black, H. R., Cushman, W. C., Green, L. A., Izzo, J. L., Jones, D. W., Materson, B. J., Oparil, S., Wright, J. T., & Roccella, E. J. (2003). Seventh report of the Joint National Committee on Prevention, Detection, Evaluation, and Treatment of High Blood Pressure. In *Hypertension* (Vol. 42, Issue 6). https://doi.org/10.1161/01.HYP.0000107251.49515.c2

Chung, E., Chen, G., Alexander, B., & Cannesson, M. (2013). Non-invasive continuous blood pressure monitoring: A review of current applications. In *Frontiers of Medicine in China* (Vol. 7, Issue 1). https://doi.org/10.1007/s11684-013-0239-5

Dixie EMS. (n.d.). *Dixie EMS Aneroid Sphygmomanometer Blood Pressure Cuff*. Retrieved August 3, 2023, from https://dixieems.com/products/dixie-child-size-pocket-aneroid-sphygmomanometer?variant=43043179036910

Downey, C. L., Chapman, S., Randell, R., Brown, J. M., & Jayne, D. G. (2018). The impact of continuous versus intermittent vital signs monitoring in hospitals: A systematic review and narrative synthesis. In *International Journal of Nursing Studies* (Vol. 84). https://doi.org/10.1016/j.ijnurstu.2018.04.013

Drzewiecki, G., Hood, R., & Apple, H. (1994). Theory of the oscillometric maximum and the systolic and diastolic detection ratios. *Annals of Biomedical Engineering*, *22*(1). https://doi.org/10.1007/BF02368225

Dynarex. (n.d.). *Digital Blood Pressure Monitor*. Retrieved August 3, 2023, from https://dynarex.com/base-digital-blood-pressure-monitors.html

Eguchi, K., Kuruvilla, S., Ogedegbe, G., Gerin, W., Schwartz, J. E., & Pickering, T. G. (2009). What is the optimal interval between successive home blood pressure readings using an automated oscillometric device? *Journal of Hypertension*, *27*(6). https://doi.org/10.1097/HJH.0b013e32832a6e39

Elegoo. (n.d.). *ELEGOO Nano V3.0 Compatible With Arduino IDE (X3)*. Retrieved August 3, 2023, from https://www.elegoo.com/products/elegoo-nano-v3-0

Forouzanfar, M., Dajani, H. R., Groza, V. Z., Bolic, M., Rajan, S., & Batkin, I. (2015). Oscillometric blood pressure estimation: Past, present, and future. *IEEE Reviews in Biomedical Engineering*, *8*. https://doi.org/10.1109/RBME.2015.2434215

Fortin, J., Rogge, D. E., Fellner, C., Flotzinger, D., Grond, J., Lerche, K., & Saugel, B. (2021). A novel art of continuous noninvasive blood pressure measurement. *Nature Communications*, *12*(1). https://doi.org/10.1038/s41467-021-21271-8

Franklin, S. S., Larson, M. G., Khan, S. A., Wong, N. D., Leip, E. P., Kannel, W. B., & Levy, D. (2001). Does the relation of blood pressure to coronary heart disease risk change with aging?: The Framingham Heart Study. *Circulation*, *103*(9). https://doi.org/10.1161/01.CIR.103.9.1245

Fuchs, F. D., & Whelton, P. K. (2020). High Blood Pressure and Cardiovascular Disease. In *Hypertension* (Vol. 75, Issue 2). https://doi.org/10.1161/HYPERTENSIONAHA.119.14240

Geddes, L. A., Voelz, M., Combs, C., Reiner, D., & Babbs, C. F. (1982). Characterization of the oscillometric method for measuring indirect blood pressure. *Annals of Biomedical Engineering*, *10*(6). https://doi.org/10.1007/BF02367308

Green, B. B., Anderson, M. L., Cook, A. J., Ehrlich, K., Hall, Y. N., Hsu, C., Joseph, D., Klasnja, P., Margolis, K. L., McClure, J. B., Munson, S. A., & Thompson, M. J. (2022).

Clinic, Home, and Kiosk Blood Pressure Measurements for Diagnosing Hypertension: a Randomized Diagnostic Study. *Journal of General Internal Medicine*, *37*(12). https://doi.org/10.1007/s11606-022-07400-z

Johns Hopkins. (2017). Vital Signs (Body Temperature, Pulse Rate, Respiration Rate, Blood Pressure) | Johns Hopkins Medicine Health Library. In © *The Johns Hopkins University, The Johns Hopkins Hospital, and Johns Hopkins Health System. All rights reserved.*

Lee, B., Jeong, J. H., Hong, J., & Park, Y. H. (2022). Correlation analysis of human upper arm parameters to oscillometric signal in automatic blood pressure measurement. *Scientific Reports*, *12*(1). https://doi.org/10.1038/s41598-022-24264-9

Leenen, J. P. L., Leerentveld, C., van Dijk, J. D., van Westreenen, H. L., Schoonhoven, L., & Patijn, G. A. (2020). Current evidence for continuous vital signs monitoring by wearable wireless devices in hospitalized adults: Systematic review. In *Journal of Medical Internet Research* (Vol. 22, Issue 6). https://doi.org/10.2196/18636

Lewis, P. S., Chapman, N., Chowienczyk, P., Clark, C., Denver, E., Lacy, P., Martin, U., McManus, R., Neary, A., & Sheppard, J. (2019). Oscillometric measurement of blood pressure: a simplified explanation. A technical note on behalf of the British and Irish Hypertension Society. In *Journal of Human Hypertension* (Vol. 33, Issue 5). https://doi.org/10.1038/s41371-019-0196-9

Mauck, G. W., Smith, C. R., Geddes, L. A., & Bourl, J. D. (1980). The meaning of the point of maximum oscillations in cuff pressure in the indirect measurement of blood pressure-part II. *Journal of Biomechanical Engineering*, *102*(1). https://doi.org/10.1115/1.3138195

McDaniel, L. M., & Ralston, S. L. (2022). How Routine are Routine Vital Signs? *Hospital Pediatrics*, *12*(7). https://doi.org/10.1542/hpeds.2021-006505

MEMSensing Microsystems. (n.d.). *Electronic blood pressure monitor pressure sensor*. MEMSensing. Retrieved August 3, 2023, from https://en.memsensing.com/product/198.html

Microchip. (n.d.). *ATmega328*. Retrieved August 3, 2023, from https://www.microchip.com/en-us/product/atmega328

Mukkamala, R., Hahn, J. O., Inan, O. T., Mestha, L. K., Kim, C. S., Toreyin, H., & Kyal, S. (2015). Toward Ubiquitous Blood Pressure Monitoring via Pulse Transit Time: Theory and Practice. *IEEE Transactions on Biomedical Engineering*, *62*(8). https://doi.org/10.1109/TBME.2015.2441951

Muntner, P., Einhorn, P. T., Cushman, W. C., Whelton, P. K., Bello, N. A., Drawz, P. E., Green, B. B., Jones, D. W., Juraschek, S. P., Margolis, K. L., Miller, E. R., Navar, A. M., Ostchega, Y., Rakotz, M. K., Rosner, B., Schwartz, J. E., Shimbo, D., Stergiou, G. S., Townsend, R. R., … Appel, L. J. (2019). Blood Pressure Assessment in Adults in Clinical Practice and Clinic-Based Research: JACC Scientific Expert Panel. In *Journal of the American College of Cardiology* (Vol. 73, Issue 3). https://doi.org/10.1016/j.jacc.2018.10.069

Muntner, P., Shimbo, D., Carey, R. M., Charleston, J. B., Gaillard, T., Misra, S., Myers, M. G., Ogedegbe, G., Schwartz, J. E., Townsend, R. R., Urbina, E. M., Viera, A. J., White, W. B., & Wright, J. T. (2019). Measurement of blood pressure in humans: A scientific statement from the american heart association. *Hypertension, 73*(5). https://doi.org/10.1161/HYP.0000000000000087

Nguyen, Y., & Bora, V. (2023, March 19). *Arterial Pressure Monitoring*. StatPearls [Internet].

Ogedegbe, G., & Pickering, T. (2010). Principles and Techniques of Blood Pressure Measurement. In *Cardiology Clinics* (Vol. 28, Issue 4). https://doi.org/10.1016/j.ccl.2010.07.006

Olshansky, B., Ricci, F., & Fedorowski, A. (2022). Importance of resting heart rate. In *Trends in Cardiovascular Medicine*. https://doi.org/10.1016/j.tcm.2022.05.006

Palatini, P., & Asmar, R. (2018). Cuff challenges in blood pressure measurement. *Journal of Clinical Hypertension, 20*(7). https://doi.org/10.1111/jch.13301

Palatini, P., Asmar, R., O'Brien, E., Padwal, R., Parati, G., Sarkis, J., & Stergiou, G. (2020). Recommendations for blood pressure measurement in large arms in research and clinical practice: Position paper of the European society of hypertension working group on blood pressure monitoring and cardiovascular variability. *Journal of Hypertension*, *38*(7). https://doi.org/10.1097/HJH.0000000000002399

Pickering, T. G., Hall, J. E., Appel, L. J., Falkner, B. E., Graves, J., Hill, M. N., Jones, D. W., Kurtz, T., Sheps, S. G., & Roccella, E. J. (2005). Recommendations for blood pressure measurement in humans and experimental animals: Part 1: Blood pressure measurement in humans - A statement for professionals from the Subcommittee of Professional and Public Education of the American Heart Association Council on high blood pressure research. In *Circulation* (Vol. 111, Issue 5). https://doi.org/10.1161/01.CIR.0000154900.76284.F6

Picone, D. S., Padwal, R., Campbell, N. R. C., Boutouyrie, P., Brady, T. M., Olsen, M. H., Delles, C., Lombardi, C., Mahmud, A., Meng, Y., Mokwatsi, G. G., Ordunez, P., Phan, H. T., Pucci, G., Schutte, A. E., Sung, K. C., Zhang, X. H., & Sharman, J. E. (2020). How to check whether a blood pressure monitor has been properly validated for accuracy. In *Journal of Clinical Hypertension* (Vol. 22, Issue 12). https://doi.org/10.1111/jch.14065

Prgomet, M., Cardona-Morrell, M., Nicholson, M., Lake, R., Long, J., Westbrook, J., Braithwaite, J., & Hillman, K. (2016). Vital signs monitoring on general wards: Clinical staff perceptions of current practices and the planned introduction of continuous monitoring technology. *International Journal for Quality in Health Care*, *28*(4). https://doi.org/10.1093/intqhc/mzw062

Raamat, R., Jagomägi, K., Talts, J., & Kivastik, J. (2013). A model-based retrospective analysis of the fixed-ratio oscillometric blood pressure measurement. *13th IEEE International Conference on BioInformatics and BioEngineering, IEEE BIBE 2013*. https://doi.org/10.1109/BIBE.2013.6701577

Rastegar, S., GholamHosseini, H., & Lowe, A. (2019). Non-invasive continuous blood pressure monitoring systems: current and proposed technology issues and challenges. In *Australasian Physical and Engineering Sciences in Medicine*. https://doi.org/10.1007/s13246-019-00813-x

Roerecke, M., Kaczorowski, J., & Myers, M. G. (2019). Comparing Automated Office Blood Pressure Readings with Other Methods of Blood Pressure Measurement for Identifying Patients with Possible Hypertension: A Systematic Review and Meta-analysis. *JAMA Internal Medicine*, *179*(3). https://doi.org/10.1001/jamainternmed.2018.6551

Sainas, G., Milia, R., Palazzolo, G., Ibba, G., Marongiu, E., Roberto, S., Pinna, V., Ghiani, G., Tocco, F., & Crisafulli, A. (2016). Mean blood pressure assessment during post-exercise: Result from two different methods of calculation. *Journal of Sports Science and Medicine*, *15*(3).

Sharma, M., Barbosa, K., Ho, V., Griggs, D., Ghirmai, T., Krishnan, S., Hsiai, T., Chiao, J.-C., & Cao, H. (2017). Cuff-Less and Continuous Blood Pressure Monitoring: A Methodological Review. *Technologies*, *5*(2). https://doi.org/10.3390/technologies5020021

Sharman, J. E., Tan, I., Stergiou, G. S., Lombardi, C., Saladini, F., Butlin, M., Padwal, R., Asayama, K., Avolio, A., Brady, T. M., Murray, A., & Parati, G. (2023). Automated 'oscillometric' blood pressure measuring devices: how they work and what they measure. In *Journal of Human Hypertension* (Vol. 37, Issue 2). https://doi.org/10.1038/s41371-022-00693-x

Shevchenko, Y. L., & Tsitlik, J. E. (1996). 90th Anniversary of the development by Nikolai S. Korotkoff of the auscultatory method of measuring blood pressure. *Circulation*, *94*(2). https://doi.org/10.1161/01.CIR.94.2.116

Stergiou, G. S., Alpert, B., Mieke, S., Asmar, R., Atkins, N., Eckert, S., Frick, G., Friedman, B., Graßl, T., Ichikawa, T., Ioannidis, J. P., Lacy, P., McManus, R., Murray, A., Myers, M., Palatini, P., Parati, G., Quinn, D., Sarkis, J., … O'Brien, E. (2018). A Universal Standard for the Validation of Blood Pressure Measuring Devices. *Hypertension*, *71*(3). https://doi.org/10.1161/hypertensionaha.117.10237

Stergiou, G. S., O'Brien, E., Myers, M., Palatini, P., Parati, G., Kollias, A., Birmpas, D., Kyriakoulis, K., Bountzona, I., Stambolliu, E., Anagnostopoulos, I., Karpettas, N., Menti, A., Asmar, R., de la Sierra, A., de Leeuw, P., Dolan, E., Head, G., Imai, Y., … Weber, M. (2019). STRIDE BP international initiative for accurate blood pressure measurement: Systematic review of published validation studies of blood pressure measuring devices. In *Journal of Clinical Hypertension* (Vol. 21, Issue 11). https://doi.org/10.1111/jch.13710

Strandberg, T. E., & Pitkala, K. (2003). What is the most important component of blood pressure: Systolic, diastolic or pulse pressure? In *Current Opinion in Nephrology and Hypertension* (Vol. 12, Issue 3). https://doi.org/10.1097/00041552-200305000-00011

Titan Micro Electronics. (n.d.). *TM7711*. Retrieved August 3, 2023, from http://www.titanmec.com/product/industrial-control/analog/20220817155.html

Whelton, P. K., Carey, R. M., Aronow, W. S., Casey, D. E., Collins, K. J., Himmelfarb, C. D., DePalma, S. M., Gidding, S., Jamerson, K. A., Jones, D. W., MacLaughlin, E. J., Muntner, P., Ovbiagele, B., Smith, S. C., Spencer, C. C., Stafford, R. S., Taler, S. J., Thomas, R. J., Williams, K. A., … Wright, J. T. (2018). 2017 ACC/AHA/AAPA/ABC/ACPM/AGS/APhA/ASH/ ASPC/NMA/PCNA guideline for the prevention, detection, evaluation, and management of high blood pressure in adults: Executive summary: A report of the American college of cardiology/American Heart Association task force on clinical practice guidelines. In *Hypertension* (Vol. 71, Issue 6). https://doi.org/10.1161/HYP.0000000000000066

Whelton, P. K., Carey, R. M., Aronow, W. S., Ovbiagele, B., Casey, D. E., Smith, S. C., Collins, K. J., Spencer, C. C., Himmelfarb, C. D., Stafford, R. S., Depalma, S. M., Taler, S. J., Gidding, S., Thomas, R. J., Jamerson, K. A., Williams, K. A., Jones, D. W., Williamson, J. D., Maclaughlin, E. J., … Mauri, L. (2017). 2017 Guideline for the Prevention, Detection, Evaluation, and Management of High Blood Pressure in Adults A Report of the American College of Cardiology/The American Heart Association. In *Journal of American College of Cardiology* (Vol. 71, Issue 6).

Yi, Z., Zhang, W., & Yang, B. (2022). Piezoelectric approaches for wearable continuous blood pressure monitoring: A review. In *Journal of Micromechanics and Microengineering* (Vol. 32, Issue 10). https://doi.org/10.1088/1361-6439/ac87ba

Zheng, D., Amoore, J. N., Mieke, S., Smith, F. E., King, S. T., & Murray, A. (2009). Automated blood pressure measurement: Reasons for measurement variability uncovered. *Computers in Cardiology, 36*.